



Article

# Soil Microbial Responses to Aflatoxin Exposure: Consequences for Biomass, Activity and Catabolic Functionality

Julius Albert , Camilla More, Sven Korz and Katherine Muñoz \*

iES Landau, Institute for Environmental Sciences, University of Kaiserslautern-Landau, 76829 Landau, Germany  
\* Correspondence: k.munoz@rptu.de

**Abstract:** Aflatoxins (AFs) are fungal secondary metabolites frequently detected in soil that exhibit in vitro toxicity to certain soil microorganisms. However, microbial responses at different levels and in complex systems such as the soil environment have not been systematically studied. Therefore, we investigated multiple microbial responses in two different soils (sandy loam and clay) to aflatoxin B1 (AFB1) at environmentally relevant concentrations ( $0.5\text{--}500 \mu\text{g kg}^{-1}$ ) during a 28-day incubation. General microbial parameters for biomass (microbial biomass carbon and ergosterol), activity (glucose-induced and basal respiration), and catabolic functionality (substrate utilization patterns) were assessed. We observed minor and transient effects in both soils. In sandy loam, we found negative effects on activity and catabolic functionality with increased metabolic quotient, while clay soil exhibited stimulation for the same parameters, suggesting a hormetic effect due to reduced bioavailability through sorption onto clay minerals. Our results indicate that AFB1 does not pose a threat to general microbial indicators under the test conditions in soils without previous AF contamination. Given the toxic potential of AFs to specific microorganisms, further studies should investigate responses at higher taxonomic and functional levels in natural environments of aflatoxigenic fungi, such as tropical soils, and including additional physicochemical stressors.

**Keywords:** aflatoxin; effects; soil microbial activity; soil microbial biomass; catabolic functionality



**Citation:** Albert, J.; More, C.; Korz, S.; Muñoz, K. Soil Microbial Responses to Aflatoxin Exposure: Consequences for Biomass, Activity and Catabolic Functionality. *Soil Syst.* **2023**, *7*, 23. <https://doi.org/10.3390/soilsystems7010023>

Academic Editor: Michael Schloter

Received: 20 January 2023

Revised: 1 March 2023

Accepted: 7 March 2023

Published: 9 March 2023



**Copyright:** © 2023 by the authors. Licensee MDPI, Basel, Switzerland. This article is an open access article distributed under the terms and conditions of the Creative Commons Attribution (CC BY) license (<https://creativecommons.org/licenses/by/4.0/>).

## 1. Introduction

Aflatoxins (AFs) are toxic secondary metabolites synthesized by certain fungal strains of the anamorph genus *Aspergillus*. Aflatoxigenic fungi naturally occur in a wide variety of environmental matrices, including soil and plant residues [1–4] and AF concentrations ranging from  $10^{-2}$  to  $10^2 \mu\text{g kg}^{-1}$  have been reported [1]. The major part of the life cycle of *Aspergilli* fungi takes place in the soil as they do not only colonize living plant tissue, but also grow saprophytically on plant debris [5]. These habitats serve as a reservoir for the fungus, allowing it to overwinter, and under favorable conditions resume growth with the potential to infest plants and crops [2,5]. In soil and decaying vegetation, these toxicogenic fungi can produce AFs, thus introducing AFs into the soil [1,6]. In addition, agricultural activities such as the incorporation of contaminated crop residues and manure [7–10] may result in inputs of aflatoxigenic fungi and AFs into the soil system beyond the natural levels. It has been reported that the soil microbiome and its associated functions can be impacted by the presence of natural toxins, including plant secondary metabolites such as phenolic compounds [11–13]. Thus, the introduction of AFs to the soil has the potential to alter the ecological balance and pose a risk to the integrity of the soil microbiome and thus to soil health [14].

In the establishment and growth of mycotoxin-producing fungi in the soil, they compete with other living organisms for the same resources [6]. The production of AFs could be a response to this microbial competition and thus part of the ecological strategy of aflatoxigenic fungi. This is supported by the fact that sclerotia and conidia spores, the structures that have to survive in the soil for a long time, have a particularly high concentration of

AFs [15]. Furthermore, increased in vitro AFs production was observed in the presence of competing soil microbes, including Gram-positive bacteria, Gram-negative bacteria, yeasts and filamentous fungi [16–18]. Other studies have shown that the production of AFs was unaffected, decreased, or even completely inhibited in the presence of filamentous fungi and Gram-positive bacteria [16,18]. Agricultural practice can significantly increase the AF level in soils beyond natural levels, with the potential to affect the soil microbiome and the soil functions it provides, thus altering the ecological balance of the soil [6,14].

The microbial response to a chemical exposure can be investigated at multiple scales. First, the response can be tested in vitro by exposing the test organism directly to the chemical stressor and excluding influencing factors such as the natural environment. In this regard, growth inhibition was observed for some Gram-positive bacteria including *Bacillus*, *Nocardia*, *Clostridium*, and *Streptomyces* in agar media supplemented with AFs (30 and 100 mg L<sup>-1</sup>), while other common Gram-positive and Gram-negative bacteria, fungi, algae, and protozoa were unaffected [19,20]. However, the tested concentrations are well above observed levels in contaminated agricultural commodities [1]. At concentrations closer to environmental levels, Angle and Wagner [21] observed inhibitory effects on native soil microorganism in two experiments: First, they observed a continuous decrease of 34–38% in the propagules of viable fungal, bacterial, and actinomycetes populations isolated from a uncontaminated silt loam soil and cultured in agar medium spiked with 1, 100, 1000, and 10,000 µg AFB1 L<sup>-1</sup> compared to the control. Next, they observed negative effects for the viable fungal, bacterial, and actinomycetes populations isolated from a AFB1 contaminated silt loam soil (1, 100, 1000, 10,000 µg AFB1 kg<sup>-1</sup>) that were cultured in agar medium. These effects occurred after two weeks of exposure and persisted for nearly six weeks. However, both the concentrations and conditions for the microbes tested using in vitro laboratory tests may not be representative of the conditions they encounter in their natural habitat, i.e., the soil environment [22].

Although in vitro studies provide key evidence on specific responses, they may not be representative of complex environmental systems since other influencing external factors are excluded [22]. In addition, less than 1% of the total microbiome can be cultured on agar media [23]. For the soil microbiome, the study of such responses should include the soil as a whole and evaluate responses at multiple levels [24]. How the microbial biomass and its composition change over the course of AF exposure in the soil has not yet been systematically investigated. The microbial response may manifest itself in the altered physiology of the microbiome, e.g., respiratory activity and substrate utilization efficiency. In this context, Angle and Wagner [21] found a significant reduction in the basal respiration rate (i.e., microbial CO<sub>2</sub> production without substrate addition) of the soil microbiome at the highest AFB1 level of 10,000 µg AFB1 kg<sup>-1</sup>, as compared to the control. At lower levels, respiration was not significantly different from the control. Basal respiration is mainly determined by substrate availability in soil, but also depends on physiological status and microbial maintenance requirements. Therefore, basal respiration can be considered as an indicator of integrated metabolic activity, but not of active microbial biomass, as it only captures the respiration of currently active microbes [25]. The application of a readily available substrate (such as glucose) prior to respiration measurement (substrate-induced respiration) stimulates a large fraction of the inactive microbiome, so that the respiratory response of the original soil microbial biomass can be investigated [26]. The microbial response to AF exposure may be reflected in a change in the catabolic functionality of the microbiome, which can be evaluated by carbon source utilization patterns [27,28]. Thereby, the quantity of utilized carbon sources reflects the abundance of microbial biomass that is able to utilize the corresponding carbon source [29]. It is assumed that the range of carbon sources utilized reflects the functional diversity of the microbial community [30]. The application of antibiotics to selectively inhibit fungi, prior to substrate-induced respiration, allows the investigation of the response of the fungal fraction of the microbiome [27,31,32].

The aim of the present study was to systematically investigate the soil microbial responses due to AF exposure at different levels, including the biomass, activity and

catabolic functionality. Furthermore, the extent to which these effects are influenced by physicochemical soil parameters was also investigated. For this purpose, sandy loam and clay soil were contaminated with AFB1 ranging from 0.5 to 500  $\mu\text{g kg}^{-1}$  and then incubated for 28 days. At discrete time points, different soil microbial parameters were assessed: total microbial biomass (via the chloroform-fumigation–extraction method), total fungal biomass (via the biomarker ergosterol), and substrate utilization patterns of the total microbial (MicroResp) and fungal communities (FungiResp). Microbial and ecophysiological ratios were calculated to detect changes in the composition or physiological state of the microbial community [24,25]. Due to the known toxicity of AFB1 on soil microbes [19–21], we expect (i) a dose-driven reduction in the microbial biomass carbon ( $C_{\text{mic}}$ ) and fungal biomass marker ergosterol (ERG), and overall reduction in multiple-substrate-induced respiration for the whole microbial and fungal communities. Since AFB1 is more toxic to soil bacteria than fungi [19,20], we expect (ii) changes in the activity and biomass composition of the microbiome towards an increase in fungal fraction. Furthermore, we hypothesize stress-induced (iii) changes in the physiological state towards an increased basal-to-substrate induced respiration ratio, increased metabolic quotients, and the reduced utilization of more complex carbon substrates. Since clay minerals strongly bind AFs [33–38], we assume that (iv) the toxic effects of AFB1 are less pronounced in the more clayey soil, as a result of reduced bioavailability.

## 2. Materials and Methods

### 2.1. Chemicals and Reagents

The AFB1 stock solution used for sample fortification was prepared by dissolving crystalline AFB1 (from *Aspergillus flavus*, Sigma-Aldrich, St. Louis, MO, USA) in acetonitrile according to the procedure described by Albert and Muñoz [39]. Ultrapure water was used throughout all work (produced by a Milli-Q-water purification system, 18.2 M $\Omega$  cm $^{-1}$ , EASYpure II, Millipore Bedford, MA, USA). Methanol (MeOH) used for ERG extraction and chromatography was of HPLC grade (Carl Roth, Karlsruhe, Germany). ERG used for external calibration was of LC grade (purity  $\geq$  95.0%, Sigma-Aldrich, Taufkirchen, Germany). The carbon substrates used for respiration experiments were D-glucose (purity  $\geq$  99.5%), D-galactose (purity  $\geq$  98%), L-alanine (purity  $\geq$  98.5%), N-acetyl-D-glucosamine (purity  $\geq$  98%),  $\alpha$ -cyclodextrin (purity  $\geq$  98%), and trisodium citrate (purity  $\geq$  99.5%), purchased from Carl Roth (Karlsruhe, Germany). The substrate  $\gamma$ -aminobutyric acid (purity  $\geq$  99%) was obtained from Sigma-Aldrich (Taufkirchen, Germany). The bacterial inhibitor bronopol (purity  $\geq$  98%) was purchased from Thermo Scientific (Schwerin, Germany).

### 2.2. Description of Test Soils

The experiments were carried out using the reference soils “RefeSol 01-A” (Fraunhofer IME, Schmallenberg, Germany) and “LUFA 6S” (LUFA, Speyer, Germany). Refesol 01-A is a strongly acidic, very light humic sandy loam soil, and LUFA 6S is a light humic and slightly alkaline clay soil (Table 1). Samples were collected from the upper layer, i.e., at 0–20 cm (LUFA 6S) and 0–25 cm (RefeSol 01-A), of organically managed arable soils from suppliers, and conditioned according to the requirements of OECD Guide 217 [40]. These soils were selected to cover a range of physicochemical properties thought to affect the bioavailability of AFB1 to soil microbes, i.e., organic carbon content, pH, and soil texture. Soil samples were prepared (removal of vegetation, larger soil organisms, and stones, and sieving through a 2 mm sieve) within one week of sampling and stored at 4 °C under aerobic and dark conditions for less than one month until use in the incubation experiments. Before conducting the main experiments, the moisture of both soils was adjusted to 40% of the maximum water holding capacity to ensure optimal microbial conditions [40]. The moisture-adjusted soils were incubated in the dark at 20 °C under aerobic conditions for 1 week to establish the equilibrium of microbial metabolism after the change from storage to incubation conditions. The total microbial biomass carbon ( $C_{\text{mic}}$ ) of the soil

microbiome prior to conducting the incubation experiment was determined using the chloroform fumigation extraction method (see Section 2.4).

**Table 1.** Physicochemical and microbial properties of the tested soils.

Property	RefeSol 01-A	LUFA 6S
Soil type	sandy loam	clay
Sand (%)	70.5	23.3
Silt (%)	26.1	35.5
Clay (%)	3.4	41.2
C <sub>org</sub> (%)	0.9	1.7
N <sub>tot</sub> (%)	0.08	0.18
WHC (%)	29.3	42.4
pH (0.01 M CaCl <sub>2</sub> )	5.4	7.3
C <sub>mic</sub> (mg kg <sup>-1</sup> )	95 ± 15	267 ± 8

### 2.3. Aflatoxin B1 Concentrations, Soil Incubation and Sampling

Incubation experiments were carried out at four AFB1 levels with 5, 50, 250 and 500 µg kg<sup>-1</sup> and a blank free of AFB1. These concentrations were chosen in line with previously reported concentrations found in soil and decaying plant material [1]. Soils were prepared according to the procedure described by Albert and Muñoz [39]. Briefly, aliquots of 3 kg soil (dry weight) were spiked by extensive shaking with AFB1-coated quartz sand (0.1–0.315 mm, acid washed) as a solid carrier at a mass ratio of 1% [40] in a securely sealed polypropylene bag. Quartz sand was coated with AFB1 using a spiking standard solution of a concentration of 500 mg L<sup>-1</sup> AFB1 in acetonitrile. Methanol was avoided as a spiking solvent to prevent the formation of artifactual methoxy species of AFB1 [41]. The solvent was allowed to evaporate for 1 h before the spiked sand was mixed with soil to avoid the potential effects of the solvent carrier on the soil microbiome [42]. The blank was prepared using the same procedure but with pure acetonitrile. Soils were then split into aliquots for the incubation experiments. For the determination of ERG and C<sub>mic</sub>, 100 g (dry weight) aliquots were incubated in 200 mL polypropylene screw-cap beakers equipped with a polyester filter floss in the cap in order to maintain aerobic conditions while minimizing the evaporation of water. To assess the microbial and fungal respiration and substrate utilization patterns as an indicator of the catabolic profile of the microbial and fungal communities, spiked or control soils were filled into 96-deep-well plates. Each plate contained a single soil at a single contamination level for a discrete sampling date. Half of the plate was then used for the analysis of the microbial catabolic profile (MicroResp) and the other half for the fungal catabolic profile (FungiResp). The filled plates were covered with Parafilm to minimize water loss while ensuring aerobic conditions. Filled incubation beakers and plates were incubated at 20 °C in the dark, and single samples were removed and analyzed at 0, 1, 3, 8, 15, 22, and 28 days of incubation. ERG and C<sub>mic</sub> contents were determined in triplicate. The respiration and catabolic profiles were assessed in duplicate. The study design and experimental workflow are shown in Figure 1.

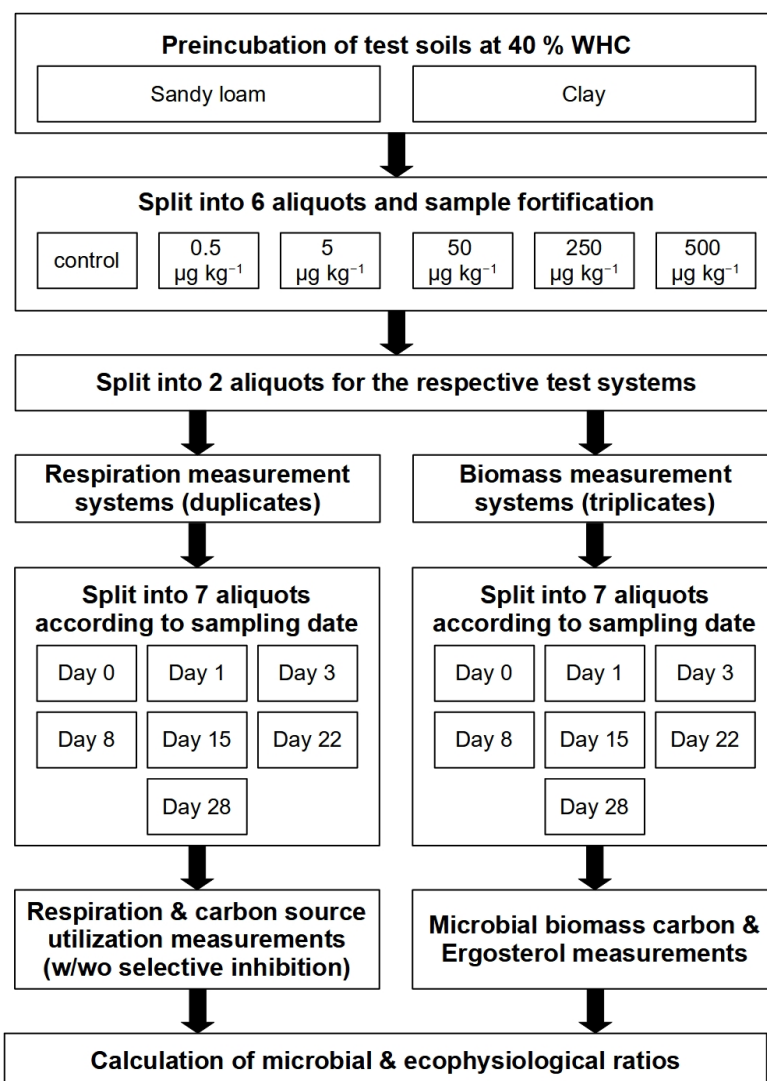


**Figure 1.** Flowchart describing the study design and experimental set up.

#### 2.4. Soil Microbial and Fungal Biomass

Soil microbial biomass carbon ( $C_{mic}$ ) was determined by the chloroform-fumigation method [43]. Briefly, fumigated (24 h, chloroform) and nonfumigated soils (20 g, fresh weight) were extracted with 80 mL of 0.5 M  $K_2SO_4$  by orbital shaking for 30 min. Extracts were filtered through a paper filter (MN 619 eh1/4, Ø: 110 mm, MACHEREY-NAGEL, Düren, Germany) and stored at  $-20^{\circ}C$  until further analysis. The filtered soil extracts were analyzed for dissolved organic carbon content with a TOC analyzer (multiNC 2011S, Analytik Jena AG, Jena, Germany). Microbial biomass carbon was calculated as the difference in carbon content between fumigated and nonfumigated values, employing a conversion factor of 0.45 [44].

The fungal cell membrane component ergosterol as an indicator of fungal biomass was extracted from soil by physical disruption according to the method described by Gong et al. [45], using a modified HPLC-UV method. Briefly, 4 g (fresh weight) of soil was extracted with 6 mL of methanol by orbital shaking (1 h, 320 rpm) in the presence of 4 g of acid-washed glass beads (2 g 212–300 µm and 2 g 710–1180 µm) followed by centrifugation at  $2190 \times g$  for 10 min. The extracts were filtered through syringe filters (0.2 µm, PET) and stored at  $-20^{\circ}C$  until measurement. HPLC analysis was performed on an Agilent 1200 series (Agilent, Santa Clara, CA, USA) system (G1311A Quaternary pump, G1322A degasser, G1329A autosampler) equipped with a column oven (Jetstream 2

column thermostat, KNAUER, Berlin, Germany) and UV detector (G1314B, Agilent, Santa Clara, CA, USA). Chromatographic separation was achieved on a LiChrospher 100 RP18 5 µm 4.6 × 250 mm column (CS Chromatographie-Service, Langerwehe, Germany) at 38 °C using isocratic elution mode, consisting of a mixture of methanol/acetonitrile (95:5, v+v) at a flow rate of 1.7 mL min<sup>-1</sup>. The injection volume was set to 100 µL. ERG was detected at an absorbance wavelength of 282 nm and quantified by external standard calibration in the range of 0.05–5 mg L<sup>-1</sup> (adj. R<sup>2</sup> = 0.999, Appendix A, Table A1). The instrumental limit of detection (LOD) and limit of quantification (LOQ), calculated according to the calibration method (DIN 32645, 2008), were 0.03 ± 0.01 and 0.09 ± 0.03 mg L<sup>-1</sup>, respectively.

## 2.5. Determination of Microbial and Fungal Respiration and Catabolic Profiles

Analysis of the substrate utilization patterns as a proxy for the catabolic profiles of soil microbial and fungal communities was performed using the miniaturized soil respiration system MicroResp, as described by Campbell et al. [28]. This method was further developed by Sassi et al. [27] into the so-called FungiResp method by using the selective bacterial inhibitor (Bronopol) to obtain the catabolic profile of the fungal fraction of the microbiome. The MicroResp method measures the microbial respiration rates induced by different carbon sources in a microplate-based respiration system [29]. Briefly, moist soil samples (adjusted to 30–60% WHC) with or without (basal respiration) carbon substrates were incubated in a 96-deep-well microplate for 6 h. CO<sub>2</sub> production was then evaluated by a pH-change-driven color reaction in an attached 96-well detection plate with agar gel containing the indicator dye cresol red [28]. This color change is proportional to the CO<sub>2</sub> evolved and is quantitatively measured by absorbance in a microplate reader at 572 nm. The following carbon sources were tested: the simple carbohydrates D-glucose and D-galactose; the amino acids L-alanine and γ-aminobutyric acid and the amino compound N-acetylglucosamine; the organic acid citric acid (as sodium citrate); and the complex carbohydrate α-cyclodextrin. These substrates were used due to their ecological relevance, their known occurrence in the soil environment (e.g., plant root exudates), and their ability to provide a sufficient range of structural complexity [46–48]. The respiratory response to the respective substrate addition reflects the proportion of active microbial biomass capable of utilizing the corresponding carbon source. Water was added to assess basal respiration. The substrates were prepared in ultrapure water at a concentration of 30 mg (g of soil water)<sup>-1</sup> [28]. The less soluble substrates (L-alanine, N-acetylglucosamine, α-cyclodextrin) were prepared as stock solutions to deliver 7.5 mg (g of soil water)<sup>-1</sup> [28]. In order to assess the respiration of the soil fungi, 25 µL of the bacterial inhibitor bronopol (dissolved in ultrapure water) was applied to the 96-deep-well microplates to achieve a nominal spiking level of 78 µg g<sup>-1</sup> (dry weight) [27]. Bronopol-spiked soils were preincubated for 1 h in order to induce sufficient inhibition prior to substrate application [27,32]. The catabolic profile of the whole microbial community was assessed by applying water instead of bronopol. After 1 h preincubation, the carbon substrates were distributed via 25 µL aliquots in a randomized block design to compensate for any edge effects on the 96-deep-well microplate [29]. Each deep-well microplate was sealed on a 96-well detection plate via a silicone seal (MicroResp, The James Hutton Institute, Dundee, UK) and incubated at 20 °C in the dark for 6 h. The absorbance of the detection plates was measured at 572 nm on an Infinite M200 plate reader (Tecan Trading AG, Männedorf, Switzerland) immediately before sealing ( $A_{t0}$ ) and after 6 h incubation ( $A_{t6}$ ). According to the manufacturer's instruction, the absorbance values were normalized by dividing the  $A_{t6}$  readings by the  $A_{t0}$  readings and multiplying them by the average  $A_{t0}$  readings obtained across all wells within each plate ( $A_i$ ).

$$A_i = \frac{A_{t6}}{A_{t0}} \times \overline{A_{t0}} \quad (1)$$

Normalized absorbance values were converted to the CO<sub>2</sub>-C air fraction by the construction of a nonlinear calibration curve. A calibration curve was constructed from

normalized absorbance values versus the headspace C-CO<sub>2</sub> air fraction obtained from the 6 h incubation of 8-well strips from a breakable microplate (12 strips of 8 wells) using gas mixtures with a known CO<sub>2</sub>-C air fraction (0.05–5%) and fitted to the inverse model provided by the manufacturer (adj. R<sup>2</sup> = 0.993, Appendix A, Table A2). The respiration rate ( $\mu\text{g CO}_2\text{-C g}^{-1}\text{ h}^{-1}$ ) was calculated by converting the 6 h CO<sub>2</sub>-C air fractions to  $\mu\text{g g}^{-1}\text{ h}^{-1}$  CO<sub>2</sub>-C using gas constants and constants for headspace volume in the well (945  $\mu\text{L}$ ), fresh weight of soil per well (g), incubation time (h), and soil sample percent dry weight according to the manufacturer's protocol.

## 2.6. Soil Microbial Indices and Ecophysiological Ratios

When assessing the impact of a chemical on the microbiome, the characterization of the community structure and physiological state of the microbial community is crucial for a more comprehensive assessment of the environmental impact of a chemical stressor [24]. The ratio of ergosterol to microbial biomass carbon ( $ERG:C_{mic}$ ) functions as an indicator for the fungal fraction of the total microbial biomass. Larger  $ERG:C_{mic}$  ratios indicate an increase in the fungal fraction within the soil microbial community.

$$ERG : C_{mic} = \frac{\text{Ergosterol}}{C_{mic}} \quad (2)$$

Similarly, respiration ratios for the basal respiration ( $BR_{fun}:BR_{mic}$ ) and the glucose-induced respiration ( $GIR_{fun}:GIR_{mic}$ ) can be calculated as an indicator fungal fraction of the total microbial activity [25]. The basal-to-substrate ratio induced respiration function ( $Q_{R,mic}, Q_{R,fun}$ ) acts as an indicator of the physiological state of the soil microbial community [25]. If the respiration rates inhibited by bronopol are used for calculation, the corresponding equivalent for the fungal fraction of the whole microbiome ( $Q_{R,fun}$ ) is obtained.

$$Q_{R,mic} = \frac{BR_{mic}}{GIR_{mic}} \quad (3)$$

$$Q_{R,fun} = \frac{BR_{fun}}{GIR_{fun}} \quad (4)$$

The ratio between basal and SIR respiration is restricted to the range between 0 and 1 and indicates the respiration ratio between growing and potentially active microorganisms. Values close to one correspond to the absence of an increase in respiratory response due to substrate addition and thus the absence of potentially active microorganisms, indicating strong suppression due to environmental stress or disturbance [25].

The metabolic quotient ( $qCO_{2,mic}$ ) is calculated from the basal respiration and microbial biomass and reflects the energetic efficiency of a microbial community. The higher the ( $qCO_{2,mic}$ ) value, the less efficient the microbial turnover as a result of a decrease in biomass and a simultaneous increase in CO<sub>2</sub>. An increase in  $qCO_{2,mic}$  is considered as an indication of stress [49–51]. Similarly, an equivalent of the metabolic quotient for the fungal fraction of the soil microbiome ( $qCO_{2,fun}$ ) can be calculated from the basal respiration inhibited by bronopol ( $BR_{fun}$ ) and the fungal biomass marker ergosterol (ERG).

$$qCO_{2,mic} = \frac{BR_{mic}}{C_{mic}} \quad (5)$$

$$qCO_{2,fun} = \frac{BR_{fun}}{Erg} \quad (6)$$

## 2.7. Data Analyses

Data processing, analyses, and visualization were conducted using R (version 4.0.3) with “tidyverse” [52] as the main package for data preparation and the “vegan” package [53] for multivariate statistics. Linear calibration curve fitting and the calculation of instrumental

LOD and LOQ were conducted with the “calibration” function implemented in the R package “envalysis” [54].

Concentration and time course effects of AFB1 on the soil microbial and ecophysiological parameters for the individual soils were investigated using multiple regression models with the continuous predictors “AFB1 concentration” and “Incubation time”. For the sandy loam soil,  $C_{mic}$  values near or below zero were found for day 0, so day 0 was excluded for the statistical analyses performed for  $C_{mic}$  and the ERG: $C_{mic}$  ratio. To test whether the effect of AFB1 concentration on the respective response variables depended on incubation time, an interaction term (“AFB1 concentration: Incubation time”) was included. For all multiple regression models, assumptions were verified by diagnostic plots [55], i.e., the criterion of (i) normality was verified via residual quantile–quantile plots, (ii) homoscedasticity via scale location plots (square root of standardized residuals versus predicted values), (iii) absence of autocorrelation via autocorrelation plots, and (iv) absence of multicollinearity via the calculation of variance inflation factors (VIF). VIF values greater than 10 were considered problematic [56]. To compensate for experimental artefacts in the MicroResp setup (e.g., edge effects) [29,57], outliers were detected and removed by the median absolute deviation (MAD) method [58]. Response variables were transformed where appropriate to meet model assumptions using frequently applied and reasonable power transformations (to the power of  $-2, -1, -0.5, 0.5, 1$ , and  $2$ ). The optimal transformation parameter was determined by the Box–Cox transformation technique [59]. Thereby, the transformation parameter closest to the best lambda value and within the confidence interval was used to perform a transformation. The test statistics for each multiple regression model are available in the Appendix (Appendix D, Table A3).

Principal response curves (PRC) [60–63] were used to assess the temporal multivariate catabolic response for each AFB1 concentration level as deviations from the nonspiked control (Appendix B). Separate principal response curve analyses were performed for each bronopol-inhibited and noninhibited soil. Monte Carlo permutation tests were conducted to assess the significance of the effects of the explanatory variable (i.e., AFB1 concentration level) on the multivariate response using an F-type statistic based on the eigenvalue of the component [60,61]. The results of the Monte Carlo permutation tests are available in the Appendix (Appendix D, Table A4).

### 3. Results and Discussion

#### 3.1. Biomass Responses to Aflatoxin Exposure

For the clay soil, a significant positive effect of AFB1 concentration ( $p < 0.001$ ) and incubation time ( $p = 0.017$ ) on  $C_{mic}$  was observed (Appendix D, Table A3, Appendix B, Figure A3). Moreover, the interaction between both concentration and time was significant ( $p = 0.004$ ), indicating that the effect of AFB1 on  $C_{mic}$  was affected by the incubation time. The  $C_{mic}$  values increased by about 67% and 377% at the highest AFB1 level ( $500 \mu\text{g kg}^{-1}$ ) from day 0 to 1 as compared to the control (Figure 2a). This effect was not further observed over the course of the incubation. For the sandy loam soil,  $C_{mic}$  content was significantly affected by incubation time ( $p = 0.003$ ) with a tendency towards increased values at the end of incubation (day 28).  $C_{mic}$  was not significantly affected by AFB1 concentration ( $p = 0.466$ ). However, at the end of incubation,  $C_{mic}$  values were reduced by about 29% (day 22) and 23% (day 28) at the highest concentration level ( $500 \mu\text{g kg}^{-1}$ ) in comparison to the control.

The clay soil showed a significant negative effect of AFB1 concentration ( $p = 0.009$ ) on ERG values, which was particularly pronounced until day 15 of incubation (Figure 2b, Appendix D, Table A3, Appendix B, Figure A3). However, at the end of incubation, ERG values were increased at the highest AFB1 concentration compared to the control. Furthermore, ERG values decreased slightly but significantly with incubation time ( $p < 0.001$ ). In the sandy loam soil, no effect of AFB1 concentration on ERG values was observed ( $p = 0.784$ ), except for day 22, where the ERG content in the control was lower than for the

highest AFB1 level ( $500 \mu\text{g kg}^{-1}$ ). However, the ERG content significantly increased over time ( $p < 0.001$ ), with levels at day 28 being approximately 60% higher than at day 0.

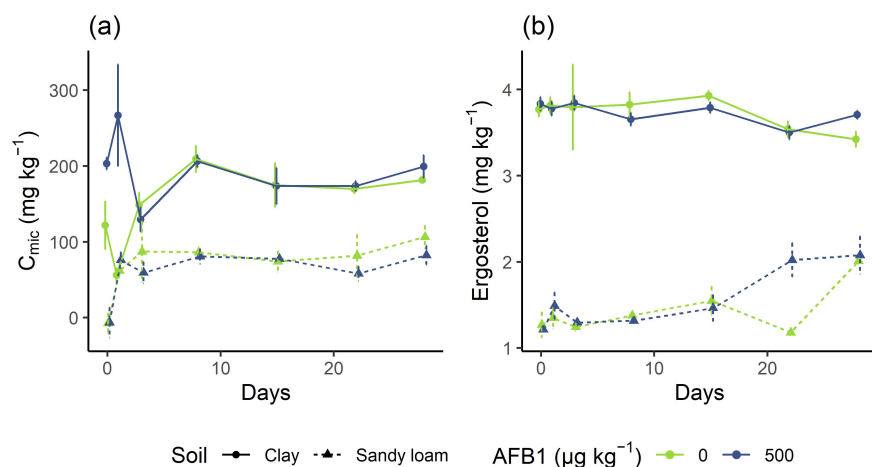


**Figure 2.** Microbial and fungal biomass responses to AFB1 exposure as a function of the incubation time. Curve plots showing the average values for microbial biomass carbon (a) and ergosterol as bioindicators for fungal biomass (b). The error bars represent the standard deviations.

It is unlikely that the AFB1-induced increase in microbial carbon biomass observed for the clay soil is due to the use of AFB1 as a carbon source to build microbial biomass, since the carbon provided by AFB1 application is multiple magnitudes lower than the increase in microbial biomass carbon. Even at the highest AFB1 dosage of  $500 \mu\text{g kg}^{-1}$  and a 100% utilization rate of AFB1 carbon for microbial growth, the increase in microbial biomass carbon could be at most  $327 \mu\text{g kg}^{-1}$ . This is much less than the observed increase in microbial biomass carbon of about  $213 \text{ mg kg}^{-1}$ . More likely, the presence of AFB1 may have affected the microbial physiological and biochemical properties and thus the fumability by chloroform and/or extractability of dissolved organic carbon released from the lysed cells. The applied AFB1 may have changed the  $\text{K}_2\text{SO}_4$  extraction recovery by desorbing dissolved organic carbon released from microbial cells from the soil matrix, resulting in a change in the measured  $C_{\text{mic}}$  independent of the actual microbial biomass [64]. AFB1 is known to have a very strong sorption affinity to clay minerals by electron–donor–acceptor interactions between the two electron-rich carbonyl groups in the coumarin structure and electron-deficient or positively charged species located at the negatively charged surface of clay minerals [33]. Furthermore, AFs strongly interact with soil organic matter with  $\log K_{\text{OC}}$  values ranging from 2.80 to 3.46 [65]. AFs with a double bond in the terminal tetrahydrofuran ring (AFB1, AFG1) have a higher sorption affinity than the saturated forms (AFB2, AFG2) [65]. This suggests that the terminal tetrahydrofuran ring is a major site of interaction with organic carbon compounds, while the coumarin ring is a site of interaction with clay mineral surfaces. In addition, nonpolar fractions of the molecule, i.e., the benzene ring and the conjugated system in the molecule, interact with aromatic fractions of the soil organic matter due to  $\pi$ – $\pi$  interactions [66,67]. Thus, the DOC molecules present in nonfumigated samples may form DOC-AFB1-clay mineral structures, resulting in lower  $\text{K}_2\text{SO}_4$  extraction efficiencies for DOC in the nonfumigated samples as a function of AFB1 concentration. In this context, the positive relationship between AFB1 concentration and dissolved organic carbon extracted from nonfumigated soils for days 0 and 1 (Appendix F, Figure A7) supports this mechanistic explanation. Furthermore, it was observed that the microbial biomass carbon calculated for day 0 in the sandy loam soil was near or below zero regardless of the AFB1 level (including the control). Because the near-zero  $C_{\text{mic}}$  observed in the control was not statistically different from the AFB1 contaminated soils, the absence of any measured microbial biomass could not be attributed to the toxic effects of AFB1. Rather, the near-zero concentrations on day 0 in the sandy loam are probably due to methodological

issues. In this regard, the extensive mixing of the soil during spiking may have resulted in cell lysis due to physical stress in the form of crushing by sand particles (sand content = 70.5%). However, such a decrease in  $C_{mic}$  at day 0 was not observed for the clay soil with a much lower sand content (23.2%). Since soil microbes strongly bind to soil clay minerals, they could be protected against these forms of physical stress in the clay soil.

Angle and Wagner [21] observed a decrease in the viable population of soil bacteria, fungi, and actinomycetes, which is in contrast to the results observed in the present study. This discrepancy may be explained by differences in the methodologies. First, in the present study, we investigated the entire microbiome in the soil as a natural habitat. In contrast, Angle and Wagner [21] either inoculated extracted soil populations in AFB1-supplemented agar media or extracted the microbial population from AFB1-fortified soil matrix by phosphate buffer extraction followed by cultivation on agar media. It is known that the majority of soil microbes (>99%) are not cultivable using conventional agar cultivation techniques [23] and, thus, the successfully cultivated microbial consortium was not representative of the total phylogenetic diversity. Hence, the toxicity observed in the study of Angle and Wagner [21] affected only a few of the species that were surveyed. Second, when using an agar plate approach, the bioavailability of AFs is likely to be much higher than in soil matrices where soil components such as clay minerals and humic substances strongly interact with AFB1 [33,65]. These methodological differences could also explain why, in the same study, almost no negative effects of AFB1 were found on the respiration of the total soil microbiome, which is generally a more sensible parameter to assess the adverse effects of a substance as it may also show nonlethal effects on soil microbes.

### 3.2. Response of Microbial Activity to Aflatoxin Exposure

Irrespective of the soil tested, no significant effect ( $p > 0.05$ ) of AFB1 concentration on the  $BR_{mic}$  and  $BR_{fun}$  was observed (Appendix D, Table A3, Appendix B, Figure A4). In addition, the  $BR_{mic}$  (Figure 3a) and  $BR_{fun}$  (Figure 3b) was not significantly affected by incubation time, except for  $BR_{fun}$  in the clay soil ( $p = 0.008$ ). However, in the clay soil,  $BR_{mic}$  and  $BR_{fun}$  values were slightly decreased at the highest spiking level ( $500 \mu\text{g kg}^{-1}$ ) compared to the control after the first week and especially at the end of incubation. Likewise, the  $GIR_{mic}$  and  $GIR_{fun}$  were not significantly affected by incubation time or AFB1 concentration in the sandy loam soil ( $p > 0.05$ , Appendix D, Table A3, Appendix B, Figure A4). In contrast, the  $GIR_{mic}$  was significantly positively affected by incubation time ( $p < 0.001$ ) and AFB1 concentration in the clay soil ( $p = 0.009$ , Figure 3c). However, the interaction between time and AFB1 concentration was significant ( $p = 0.009$ ), indicating that the effect of AFB1 on  $GIR_{mic}$  was affected by the incubation time, with a tendency for positive effects of AFB1 on  $GIR_{mic}$  at the beginning of the incubation period and slightly negative effects at the end of incubation. In this regard,  $GIR_{mic}$  and  $GIR_{fun}$  values were increased at the highest spiking level ( $500 \mu\text{g kg}^{-1}$ ) compared with the control (Figure 3c,d). For the  $GIR_{fun}$  in clay soil, no effect of AFB1 concentration was found ( $p = 0.08$ , Figure 3d).

The results of the present study are in line with Angle and Wagner [21], who observed no effect of AFB1 application at similar AFB1 fortification levels (from 1 to  $1000 \mu\text{g kg}^{-1}$ ) on the basal respiration in a silt loam soil. This can be explained by the relatively high cation exchange capacity of the silt loam soil ( $14 \text{ meq (100 g)}^{-1}$ ) [21], indicating a high content of clay minerals [68], a soil fraction that is known to strongly absorb AFs [33], reducing their bioavailability. At a fortification level of  $10,000 \mu\text{g kg}^{-1}$ , Angle and Wagner [21] observed a slightly but significantly reduced cumulative  $\text{CO}_2$  production at the end of 70 days of incubation compared to the control. This is consistent with the present study, in which baseline microbial and fungal respiration began to decrease at the end of incubation at the highest AFB1 concentration. However, these concentrations may be much higher than environmentally relevant levels [1]. Likewise, in the present study, no toxic effects were detected on glucose-induced respiration, a parameter that is much more sensitive to stress, since the provision of the easily decomposable substrate glucose activates a large fraction of the inactive microbes [25]. Moreover, microbial and fungal glucose-induced respiration

increased transiently in the first few days after AFB1 application. One explanation for this increase could be that soil microbes adapted at the cellular level for the purpose of detoxifying AFB1 by producing degradative enzymes. Thus, during AFB1 detoxification, glucose could be co-metabolized alongside with AFB1, leading to an increase in glucose-induced respiration rates. Further investigation through enzyme activity studies of soils exposed to aflatoxins could verify this hypothesis. Therefore, our results suggest that AFB1 at environmentally relevant concentrations does not have a harmful effect on the metabolic activity of the fungi and the overall microbiome.

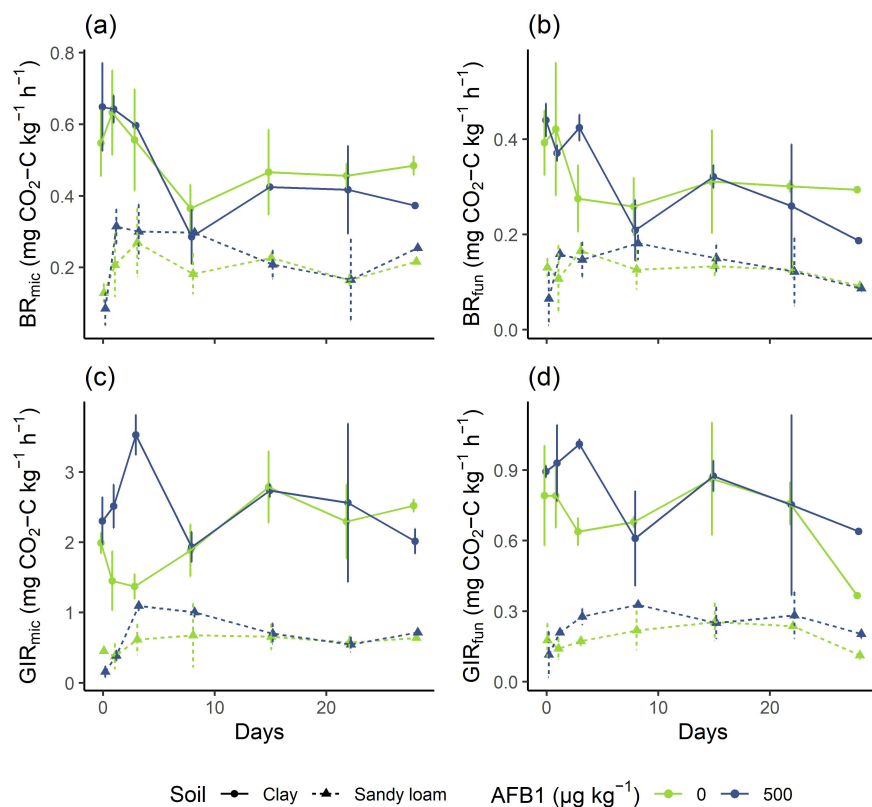


**Figure 3.** Microbial and fungal activity responses to AFB1 exposure as a function of the incubation time. Curve plots showing mean values for microbial basal respiration  $BR_{mic}$  (a), microbial glucose-induced respiration  $GIR_{mic}$  (c), fungal basal respiration  $BR_{fun}$ , and fungal glucose-induced respiration  $GIR_{fun}$  (d). The error bars represent the standard deviations.

### 3.3. Carbon Source Utilization Patterns

In clay soil, the overall microbial carbon source utilization in terms of the canonical coefficient significantly increased with AFB1 concentration until the third day ( $p = 0.03$ , Appendix D, Table A4, Figure 4). A similar situation was observed for the fungal carbon source utilization in the clay soil, although the increase was not significant ( $p = 0.296$ , Appendix D, Table A4, Figure 4). The opposite pattern was observed for the fungal carbon source utilization in the sandy loam soil, where the canonical coefficient decreased from day 1, although not significantly ( $p = 0.109$ , Appendix D, Table A4, Figure 4). After the first week, the decrease or increase in the canonical coefficient as a function of AFB1 concentration was less pronounced (Figure 4). Coincidentally, the species weights for all substrates slightly decreased in the sandy loam and slightly increased in the clay soil as compared to the control (Figure 4). In the clay soil, the respiration induced by the readily available carbon substrate glucose (in terms of species weight) was most affected by AFB1 application for both the fungal and whole microbial fungal communities. The respiration induced by all other substrates was much less affected. In sandy soil, the microbial

respiration induced by the amino acid L-alanine, the complex polymer  $\alpha$ -cyclodextrin, and glucose was affected by AFB1 application, while for fungal respiration,  $\alpha$ -cyclodextrin and glucose-induced respiration were affected (Figure 4).

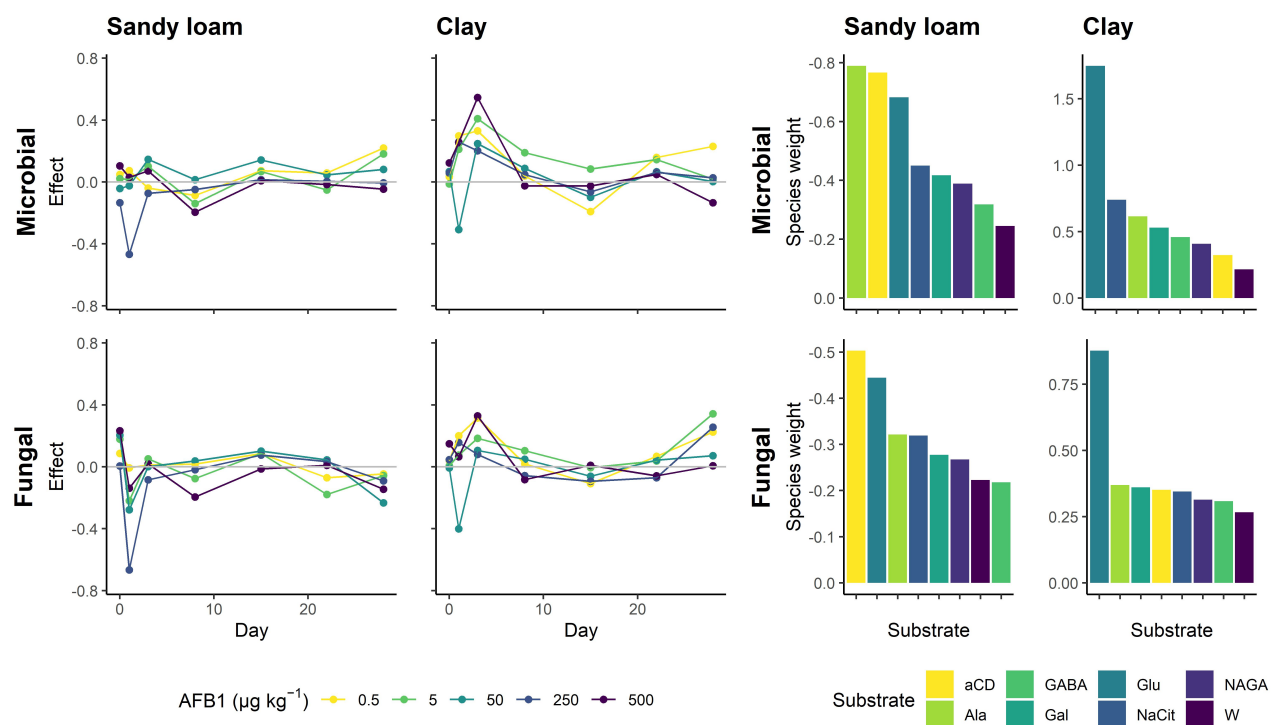


**Figure 4.** Microbial and fungal carbon source utilization patterns. Left panel: Principal response curves showing the temporal multivariate catabolic response for each AFB1 concentration level as deviations from the nonspiked control (i.e., the zero line). Right panel: Barplots showing the species weights (right) for the response of individual substrates. Glu = D-glucose, Gal = D-galactose, GABA =  $\gamma$ -aminobutyric acid, NAGA = N-acetylglucosamine, NaCit = sodium citrate, and aCD =  $\alpha$ -cyclodextrin.

Only minimal negative effects of AFB1 on fungal catabolic profiles occurred in the sandy loam soils. This indicates that overall fungal metabolism in the sandy loam was slightly reduced after AFB1 application. This may be explained by the fast decomposition of AFB1 [1,35,37,39], as reflected in a fast initial drop in extractable AFB1 content in the sandy loam [39]. Furthermore, the particularly complex biopolymer  $\alpha$ -cyclodextrin was one of the substrates with the strongest decrease in species weight due to AFB1 exposure. This is in line with our assumption that AFB1-stressed microbial communities are less capable of utilizing more complex carbon substrates. The degradation of complex structures, such as  $\alpha$ -cyclodextrin, requires a higher energy investment compared with readily available compounds, since specialized enzymes need to be produced for the decomposition of these polymers [69,70]. Thus, when microbes are exposed to a chemical stressor, they may prefer simple and readily available substrates such as glucose because the energetic gain from utilizing complex substrates such as  $\alpha$ -cyclodextrin would not justify the investment required to break down these complex substrates. To gain more comprehensive insights into these processes, enzyme assays targeting different levels of substrate complexity could be conducted. These assays would include enzymes specific to the lignin-degrading system, such as laccase (very complex substrates), polysaccharidases, such as amylases (medium-complexity substrates), and oxidoreductases such as glucose oxidase (readily available substrates). In contrast, the catabolic profile in the clay soil was positively affected until day 3, and the species weights for all substrates were positive. The distinctive pattern

in the first week suggests short-term positive effects of AFB1 on the catabolic profiles of the fungal and whole microbial community in the clay soil. These results are consistent with the increase in microbial biomass carbon observed at the beginning of the incubation experiment (Figure 2). Likewise, the unexpected stimulative effect of AFB1 for the clay soil may be explained by the strong sorption capability of clay minerals. Clay minerals are known to provide sorption sites for dissolved organic compounds (such as the substrates used in this study) [71], as well as soil microbes [72] and their extracellular secreted enzymes [73]. Due to the high sorption affinity of AFB1 to clay minerals, a displacement of these adsorbates from the clay mineral sorption sites may have occurred, as is known for other negatively charged substances such as phosphates [74,75]. A subsequent release of the absorbed substrates, microorganisms, and/or soil enzymes could then have resulted in increased CO<sub>2</sub> production. Another possible explanation for the positive short-term effect of AFB1 on the catabolic response in the clay soil could be stimulation by low available doses of AFB1, resulting in an increased catabolic response. This phenomenon has also been described for secondary metabolites such as alkaloids and is referred to as hormesis [76,77]. Hormesis refers to the beneficial effects of exposure to low doses of a stressor that is typically harmful at higher doses [76]. In the clay soil, the bioavailable AFB1 concentration could be reduced by clay mineral adsorption to be within the hormetic zone, where the metabolic response to low exposure to the chemical stressor is favorable. In the context of aflatoxin exposure, low doses may activate cellular stress response pathways that enhance the microbial ability to deal with subsequent exposure to higher doses of the stressor. Cellular adaption, e.g., the production of enzymes, may lead to the increased co-metabolization of carbon substrates and thus increased CO<sub>2</sub> production. Another explanation could be that AFs in low doses could also be beneficial to microbes by being involved in certain soil reactions themselves. In this context, Finotti, et al. [78] showed that AFs efficiently scavenge peroxides and extend the lifespan of *Escherichia coli* growing under oxidative stress conditions. The authors hypothesized that AFs function as antioxidants and their biological purpose is to extend the lifespan of aflatoxigenic fungi under highly oxidative conditions, such as when substrate resources are depleted. Therefore, the role of AFB1 as a secondary metabolite in further reactions in soils and in terms of microbial responses to stress should be further investigated.

### 3.4. Soil Microbial and Ecophysiological Ratios

The ERG:C<sub>mic</sub> significantly decreased with AFB1 concentration in the clay soil ( $p < 0.001$ ) and there was a significant decrease in the ERG:C<sub>mic</sub> ratio over time ( $p = 0.002$ , Appendix D, Table A3, Appendix B, Figure A5). The interaction between AFB1 concentration and incubation time was significant ( $p = 0.002$ , Figure 5a), indicating that the effect of AFB1 was time-dependent. Consistent with the results for C<sub>mic</sub>, the effect of AFB1 on the ERG:C<sub>mic</sub> ratio was present only at day 0 and 1, where a strong decrease of about 80% was observed at the highest concentration level (500 µg kg<sup>-1</sup>) as compared to the control. In contrast, for the sandy loam soil, the ERG:C<sub>mic</sub> ratio was neither affected by AFB1 concentration ( $p = 0.733$ ) nor by the incubation time ( $p = 0.416$ ). The fungal-to-microbial activity ratios were not affected by AFB1 concentration or by the incubation time (Figure 5b,c).

In the clay soil, both incubation time ( $p < 0.001$ ) and AFB1 concentration ( $p = 0.03$ ) had a significant negative effect on the Q<sub>R,mic</sub> (Figure 6a), while for the Q<sub>R,fun</sub> (Figure 6b), no effect of time and AFB1 concentration could be observed (Appendix D, Table A3, Appendix B, Figure A6). In the sandy soil, there were inconsistent effects of AFB1. While the fungal metabolic quotient (Figure 6d) was unaffected by AFB1 concentration ( $p = 0.67$ ), the microbial metabolic quotient (Figure 6c) was slightly but significantly increased by AFB1 ( $p = 0.045$ , Appendix D, Table A3, Appendix B, Figure A6). Furthermore, there was a significant decrease over time in the metabolic quotient for the soil fungal ( $p = 0.031$ ) and whole microbiome ( $p = 0.005$ , Appendix D, Table A3, Appendix B, Figure A6).

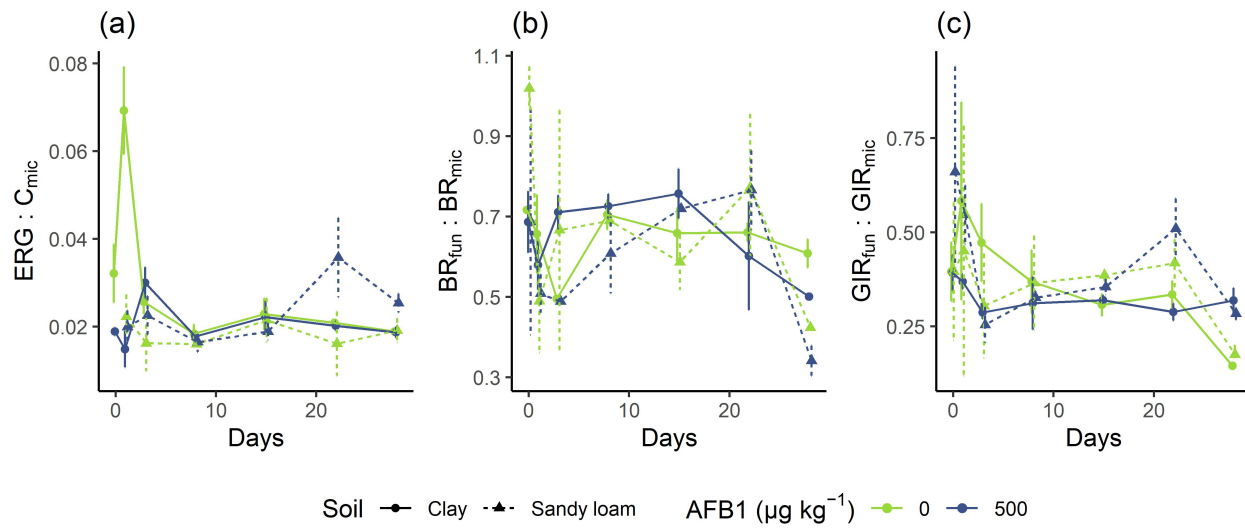


**Figure 5.** Biomass and activity ratios in AFB1-exposed ( $500 \mu\text{g kg}^{-1}$ ) and control soil as a function of incubation time. Curve plots showing fungal-to-microbial ratios for the biomass ERG:C<sub>mic</sub> (a), basal respiration BR<sub>fun</sub>:BR<sub>mic</sub> (b), and glucose-induced respiration GIR<sub>fun</sub>:GIR<sub>mic</sub> (c).

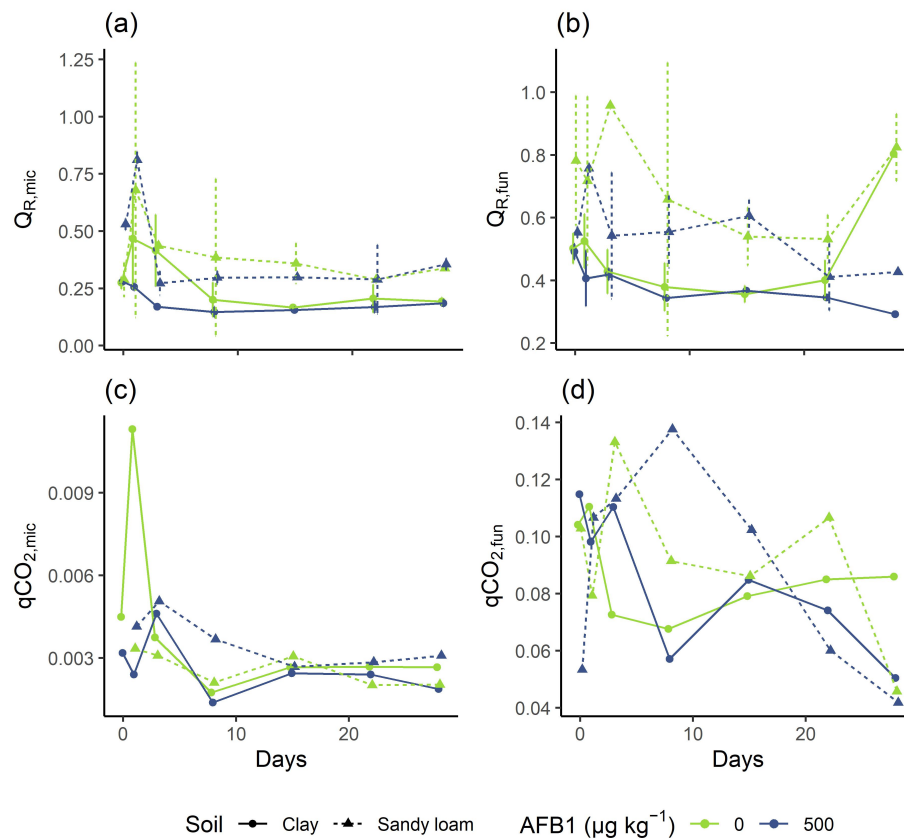


**Figure 6.** Ecophysiological ratios for AFB1-exposed ( $500 \mu\text{g kg}^{-1}$ ) and control soils as a function of incubation time. Microbial basal-to-substrate induced respiration Q<sub>R,mic</sub> (a), fungal basal-to-substrate induced respiration Q<sub>R,fun</sub> (b), microbial metabolic quotient qCO<sub>2,mic</sub> (c), and fungal metabolic quotient qCO<sub>2,fun</sub> (d).

For the clay soil, the fungal proportion in terms of ERG:C<sub>mic</sub> was strongly decreased at the beginning of incubation, in contrast to Burmeister and Hesseltine [19], who observed only limited effects of AFB1 on soil fungal species, while several bacterial species were negatively affected by AFB1. The observed short-term effect on clay soil can also be explained by methodological issues related to the determination of microbial biomass carbon rather than actual changes in soil microbial biomass, as discussed earlier. The strong decrease in the ERG:C<sub>mic</sub> ratio was driven by a strong increase in the C<sub>mic</sub> as a function of AFB1 concentration, since the ERG was not significantly affected by AFB1 concentration. For the sandy loam, no effects were observed on the fungal fraction. Likewise, the fungal contribution of the microbial basal and glucose-induced respiration was not affected by AFB1 application. Therefore, it can be assumed that the biomass and the activity of the total microbiome, as well as the soil fungi, were unaffected by AFB1. However, it should be mentioned that the methodology used to detect changes in the activity and structure of the microbial community has a relatively low resolution, as it can only discriminate between effects on fungi and the total microbiome. Methods with a better resolution would allow discrimination even at much lower taxonomic or physiological levels, e.g., quantitative PCR (qPCR) using taxon-specific primers [79] and the analysis of phospholipid fatty acids (PLFA [80,81]).

Regardless of soil, neither the ratio of fungal- nor microbial-induced basal respiration to substrate respiration was increased. Moreover, the microbial Q<sub>R,mic</sub> was significantly decreased in the clay soil, which was attributable to a significant increase in the GIR, suggesting that a proportion of the potentially active microorganisms were stimulated by AFB1 [25]. As discussed above in relation to the observed increase in catabolic response, the toxicity and/or bioavailability of AFB1 may have been reduced due to sorption to clay minerals, to the extent that a hormetic effect occurred [76]. In contrast, the microbial metabolic quotient was significantly increased in the sandy loam soil as a function of the AFB1 dose at the beginning of incubation, indicating a reduced energetic efficiency in the microbial turnover due to chemical stress [50,51]. The lack of any effect of the fungal basal-to-substrate induced respiration ratio and metabolic quotient suggests that the bacterial fraction of the soil microbiome was mainly affected by AFB1. This is consistent with previous studies, which showed that certain soil bacteria, particularly those that are Gram-positive, are the most affected group [19,20].

#### 4. Conclusions

Aflatoxin B1 has been recognized for its harmful impact on certain bacteria and fungi in *in vitro* experiments, but its effects on microbial communities in complex environmental systems such as soil have not been systematically investigated. The present study investigated, for the first time, the microbial responses against AFB1 exposure at different physiological levels including biomass, activity, and carbon source utilization patterns, taking into account the complexity of the soil as a matrix. In line with previous studies, it was shown that AFB1 at environmentally relevant concentrations had only minor and transient effects on the biomass and activity of soil microbes. Furthermore, the strength and direction of the observed effects were dependent on the soil. Thus, soil texture largely influenced AFB1 availability. Minor and transitory stimulatory effects on catabolic functionality and microbial activity were observed for clay soil. This suggests that the toxicity and availability of AFB1 was reduced by clay mineral-induced sorption and thus a hormetic effect may have occurred. In contrast, AFB1 in sandy loam soil had a minor negative effect on catabolic functionality and microbial activity, and triggered a slight increase in metabolic quotient. Overall, based on the present study, it can be concluded that AFs do not pose a threat to the integrity of the soil microbiome and thus to soil health for the concentration range and time frame tested. However, although no effects on the community structure in the form of the fungal fraction of the biomass were found, a change in the microbial composition cannot be excluded because the methodology used has only a low taxonomic and physiological resolution. In addition, the present study only investigated the effects of a single AFB1

application on German reference soils, which were presumably never exposed to AFs. Since soils from aflatoxin hotspot regions are frequently exposed to AFs, long-term effects could occur that were not investigated in the present work. Aflatoxin-exposed soils, e.g., from the (sub)tropics in Africa, may be exposed to other stressors such as pesticides, fertilizers, floods, and drought events. The interaction of these stressors with AFs could change the intensity and direction of the effects of AFs on the soil microbiome. Therefore, further studies in the natural environment of aflatoxin-producing fungi are essential to obtain a more comprehensive picture of the environmental relevance of AFs to the soil microbiome and thus soil health.

**Author Contributions:** Conceptualization, J.A. and K.M.; methodology, J.A., C.M. and S.K.; software, J.A.; validation, J.A., K.M., C.M. and S.K.; formal analysis, J.A.; investigation, J.A., K.M., C.M. and S.K.; resources, J.A. and K.M.; data curation, J.A.; writing—original draft preparation, J.A.; writing—review and editing, J.A., K.M., C.M. and S.K.; visualization, J.A.; supervision, K.M.; project administration, K.M.; funding acquisition, K.M. All authors have read and agreed to the published version of the manuscript.

**Funding:** The project is being funded by the Federal Ministry of Food and Agriculture BLE under the reference AflaZ 2816PROC14.

**Institutional Review Board Statement:** Not applicable.

**Informed Consent Statement:** Not applicable.

**Data Availability Statement:** The data that support the findings of this study are available from the corresponding author upon reasonable request.

**Conflicts of Interest:** The authors declare no conflict of interest.

## Appendix A. Calibration Figures

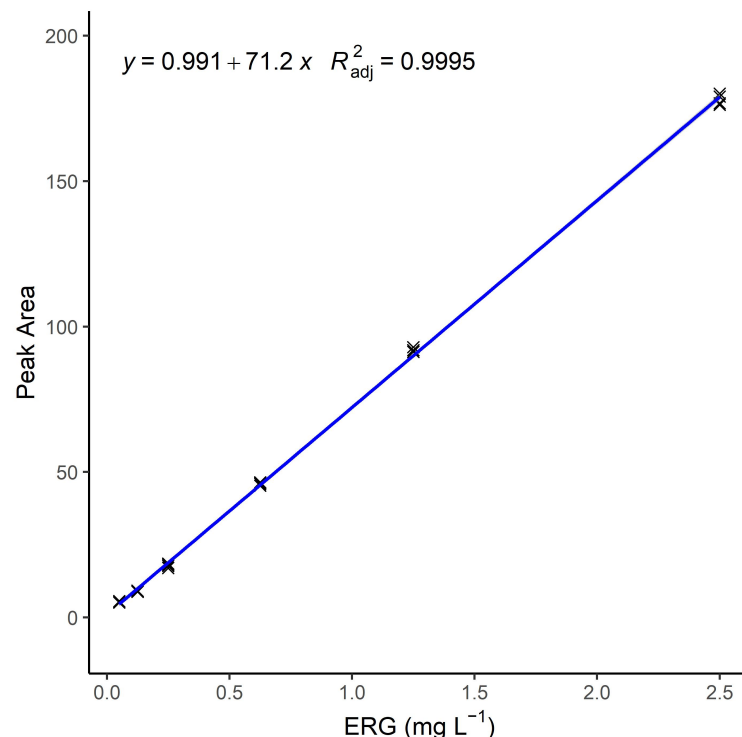


**Figure A1.** Calibration curve for ergosterol.

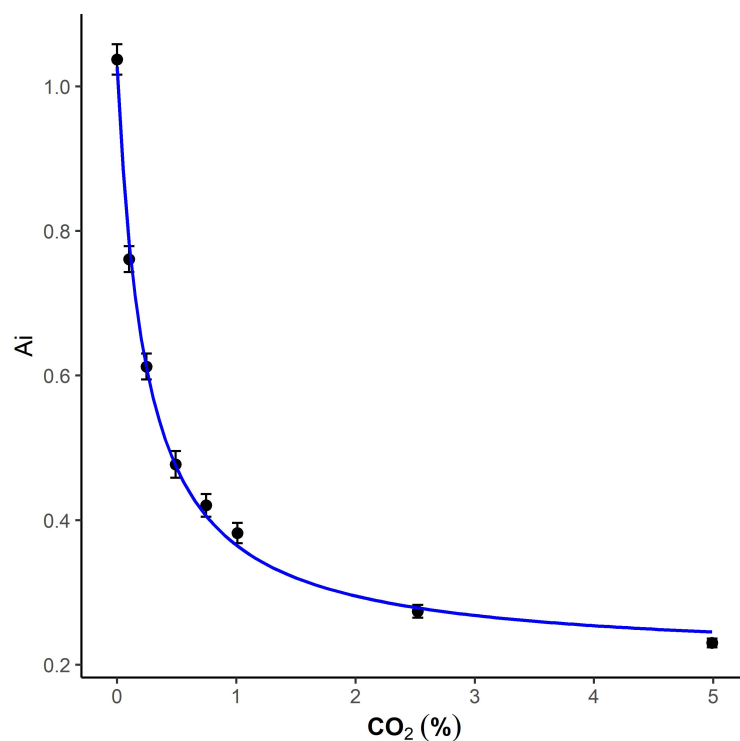


**Figure A2.** Nonlinear calibration curve for MicroResp. The x axis shows the percentage air fraction of CO<sub>2</sub> and the y axis shows the normalized absorbance at 572 nm.

#### Appendix B. Microbial Responses to Aflatoxin B1

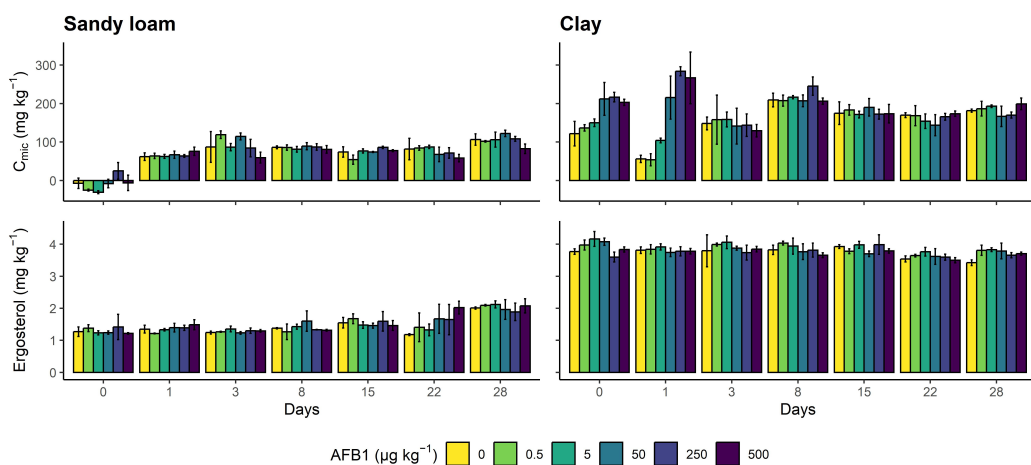


**Figure A3.** Microbial and fungal biomass: Barplots showing the average values for microbial biomass carbon (C<sub>mic</sub>) and ergosterol as bioindicators for fungal biomass (ERG). The error bars represent the standard deviations.

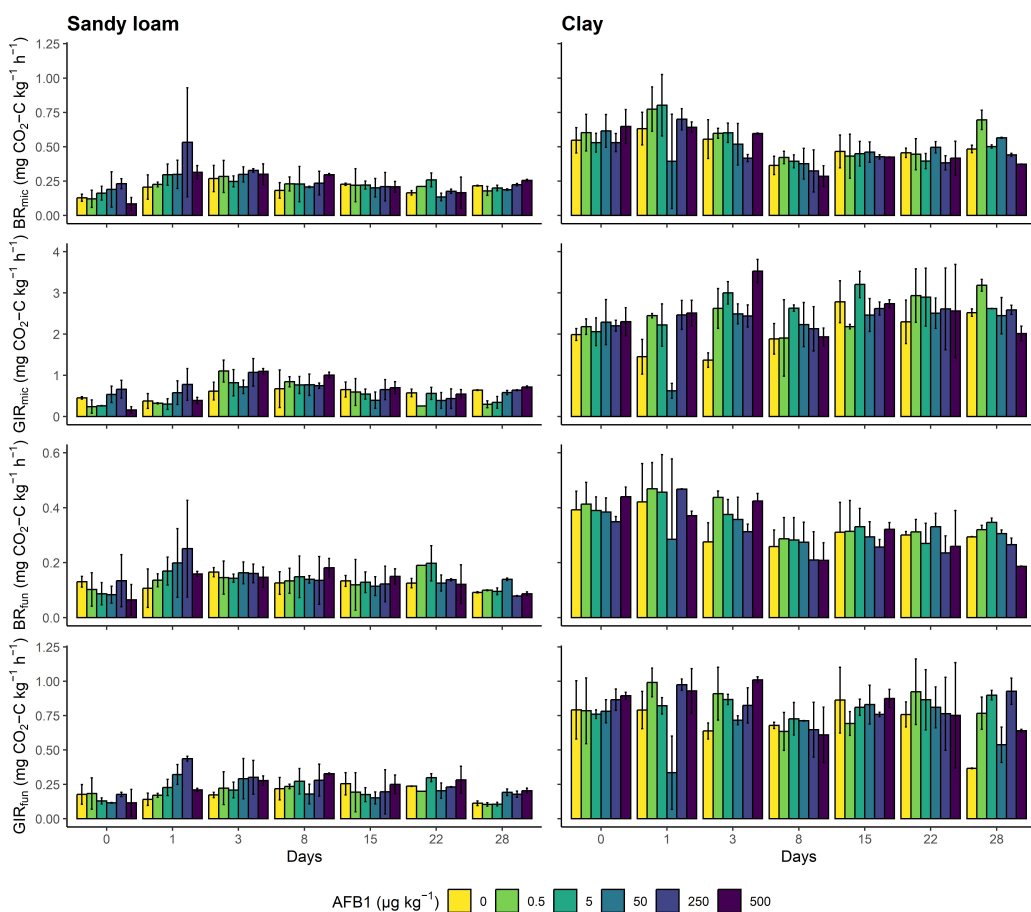


**Figure A4.** Microbial and fungal activities: Barplots showing mean values for microbial basal respiration ( $\text{BR}_{\text{mic}}$ ), microbial glucose-induced respiration ( $\text{GIR}_{\text{mic}}$ ), fungal basal respiration ( $\text{BR}_{\text{fun}}$ ), and fungal glucose-induced respiration ( $\text{GIR}_{\text{fun}}$ ). The error bars represent the standard deviations.

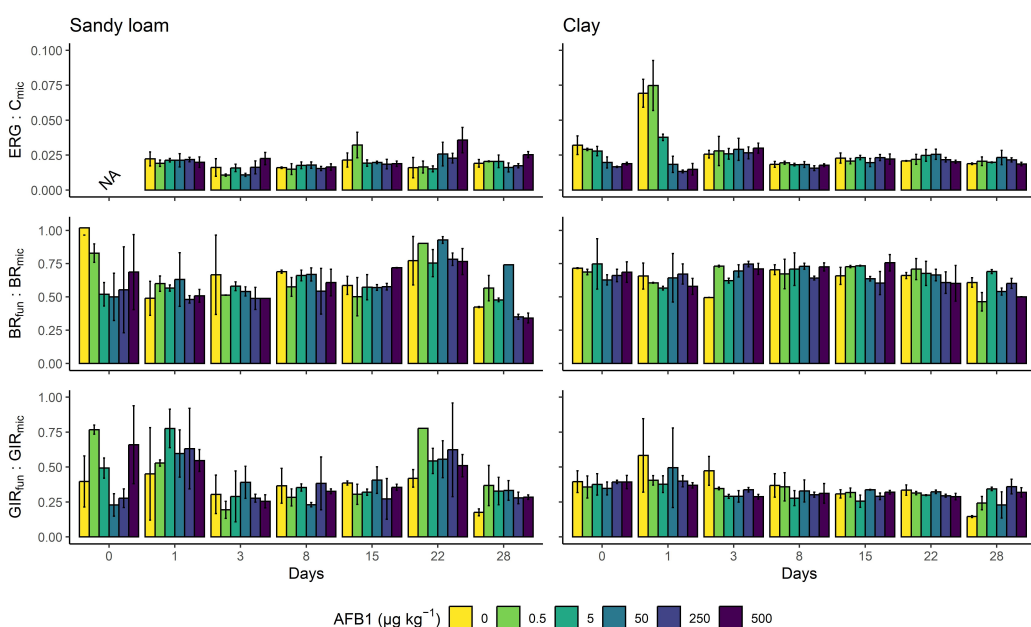


**Figure A5.** Biomass and activity ratios: Fungal-to-microbial ratios for the biomass ( $\text{ERG:C}_{\text{mic}}$ ), basal respiration ( $\text{BR}_{\text{fun}}:\text{BR}_{\text{mic}}$ ), and glucose-induced respiration ( $\text{GIR}_{\text{fun}}:\text{GIR}_{\text{mic}}$ ).

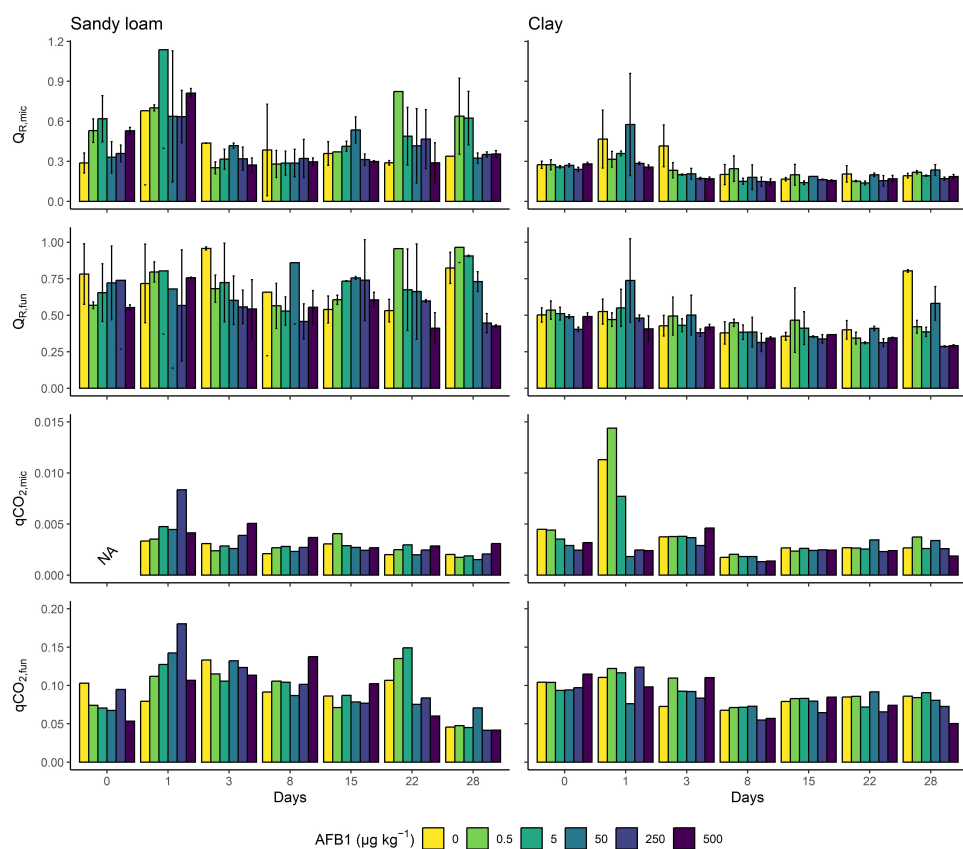


**Figure A6.** Ecophysiological ratios: Microbial basal-to-substrate induced respiration ( $Q_{R,\text{mic}}$ ), fungal basal-to-substrate induced respiration ( $Q_{R,\text{fun}}$ ), microbial metabolic quotient ( $qCO_2,\text{mic}$ ), and fungal metabolic quotient ( $qCO_2,\text{fun}$ ).

### Appendix C. Principal Component Analysis

PRC is a constrained ordination technique and a special case of redundancy analysis (RDA). A problem with traditional ordination methods such as RDA is that temporal changes in treatment effects make treatment effects (e.g., compared to a control) difficult to determine if time does not follow a straight line in the ordination graph, resulting in a cluttered and difficult-to-interpret ordination graph [60,61]. PRC overcomes this problem by focusing on the differences between the species (e.g., the respiration rates induced by the individual substrates) compositions of treatments at each sampling date [62]. For PRC construction, an RDA model is fitted to the multivariate response using treatment, time, and their interaction as predictors. Since the main interest is in the multivariate response due to treatment and not due to overall temporal change, the main effect of time is factored out and only the treatment:time interaction is kept. As a result, the RDA axes show only the change explained by treatment and the treatment:time interaction, but not the overall temporal trend [63]. The PRC plot shows on the y axis the difference in the canonical coefficient of the treatments (i.e., the individual AFB1 concentration levels) from the nonspiked control (represented graphically as a zero line), and on the x axis the incubation time. The further the communities are from the control line, the more they differ from the control group. The extraction of the accompanying species (i.e., substrates) weights allows interpretation at the species level. The higher the respective species weight, the more likely that the actual response pattern of the species follows the pattern in the PRC, while species with a highly negative weight are assumed to show the opposite pattern. Species with a weighting close to zero either show no response or a response that does not match the pattern shown by the PRC [61].

**Table A1.** Principal response curves: Differences in the canonical coefficients of the treatments (i.e., the individual AFB1 concentration levels) from the nonspiked control for both soils (sandy loam and clay) and systems (microbial and fungal) over 28 days of incubation.

Day	AFB1 ( $\mu\text{g kg}^{-1}$ )	Sandy Loam		Clay	
		Microbial	Fungal	Microbial	Fungal
0	0.5	0.048	0.086	0.034	0.04
	5	0.022	0.179	-0.013	0.007
	50	-0.042	0.204	0.067	-0.007
	250	-0.135	0.006	0.059	0.046
	500	0.104	0.233	0.124	0.15
1	0.5	0.073	-0.007	0.298	0.201
	5	0.016	-0.219	0.211	0.075
	50	-0.025	-0.278	-0.308	-0.4
	250	-0.468	-0.667	0.258	0.157
	500	0.029	-0.138	0.254	0.065
3	0.5	-0.039	0.012	0.331	0.316
	5	0.101	0.051	0.409	0.185
	50	0.146	0.002	0.248	0.106
	250	-0.073	-0.083	0.201	0.081
	500	0.072	0.019	0.545	0.329
8	0.5	-0.087	0.018	0.039	0.019
	5	-0.139	-0.076	0.19	0.104
	50	0.014	0.038	0.088	0.049
	250	-0.048	-0.019	0.047	-0.057
	500	-0.194	-0.195	-0.024	-0.082
15	0.5	0.073	0.085	-0.191	-0.108
	5	0.068	0.087	0.084	-0.006
	50	0.143	0.102	-0.099	-0.061
	250	0.014	0.076	-0.063	-0.094
	500	0.008	-0.013	-0.026	0.009
22	0.5	0.058	-0.071	0.158	0.068
	5	-0.052	-0.179	0.145	0.038
	50	0.046	0.046	0.067	0.043
	250	0.004	0.033	0.062	-0.071
	500	-0.017	0.01	0.049	-0.059
28	0.5	0.22	-0.046	0.23	0.224
	5	0.181	-0.057	0.019	0.343
	50	0.082	-0.232	0.003	0.072
	250	-0.005	-0.091	0.027	0.256
	500	-0.046	-0.145	-0.134	0.007

**Table A2.** Species weight for the principal response curves. Species represent the carbon substrates used for substrate-induced respiration measurements. Glu = D-glucose, Gal = D-galactose, GABA =  $\gamma$ -aminobutyric acid, NAGA = N-acetylglucosamine, NaCit = sodium citrate, and aCD =  $\alpha$ -cyclodextrin.

Substrate	Sandy Loam		Clay	
	Microbial	Fungal	Microbial	Fungal
aCD	-0.77	-0.5	0.32	0.35
Ala	-0.79	-0.32	0.62	0.37
GABA	-0.32	-0.22	0.46	0.31
Gal	-0.42	-0.28	0.53	0.36
Glu	-0.68	-0.44	1.75	0.88
NaCit	-0.45	-0.32	0.74	0.34
NAGA	-0.39	-0.27	0.41	0.31
W	-0.24	-0.22	0.22	0.27

## Appendix D. Test Statistics of the Multiple Regression Models

**Table A3.** Test statistics of the multiple regression models used to evaluate the effect of AFB1 concentration, incubation time and their interaction on soil microbial and ecophysiological parameters. Significant results ( $p < 0.05$ ) are shown in bold.

Response	Soil	Predictor	B	SE	t	p
$C_{\text{mic}}$	clay	Intercept	151	7.48	20.173	<b>&lt;0.001</b>
sandy loam		Time	1.2	0.5	2.41	<b>0.017</b>
		AFB1	0.147	0.0327	4.516	<b>&lt;0.001</b>
		Time:AFB1	-0.00642	0.00218	-2.942	<b>0.004</b>
		Intercept	76.7	3.74	20.513	<b>&lt;0.001</b>
		Time	0.703	0.231	3.038	<b>0.003</b>
		AFB1	-0.0119	0.0163	-0.731	0.466
		Time:AFB1	-0.00082	0.00101	-0.813	0.418
ERG		Intercept	3.93	0.0303	129.616	<b>&lt;0.001</b>
		Time	-0.00894	0.00203	-4.411	<b>&lt;0.001</b>
		AFB1	-0.00035	0.000132	-2.644	<b>0.009</b>
		Time:AFB1	$9.3 \times 10^{-6}$	$8.85 \times 10^{-6}$	1.051	0.296
		Intercept	0.788	0.0154	51.069	<b>&lt;0.001</b>
		Time	-0.00732	0.00103	-7.097	<b>&lt;0.001</b>
		AFB1	$-1.85 \times 10^{-5}$	$6.74 \times 10^{-5}$	-0.274	0.784
BR <sub>mic</sub>		Time:AFB1	$-5.43 \times 10^{-6}$	$4.5 \times 10^{-6}$	-1.205	0.231
		Intercept	0.552	0.0265	20.866	<b>&lt;0.001</b>
		Time	-0.00301	0.00177	-1.704	0.092
		AFB1	$1.2 \times 10^{-5}$	0.000115	0.104	0.918
		Time:AFB1	$-1.08 \times 10^{-5}$	$7.72 \times 10^{-6}$	-1.395	0.167
		Intercept	0.235	0.0189	12.428	<b>&lt;0.001</b>
		Time	-0.00151	0.00128	-1.18	0.241
BR <sub>fun</sub>		AFB1	$9.73 \times 10^{-5}$	$8.26 \times 10^{-5}$	1.178	0.242
		Time:AFB1	-2.66e-06	5.54e-06	-0.48	0.632
		Intercept	0.37	0.0161	22.894	<b>&lt;0.001</b>
		Time	-0.00294	0.00108	-2.722	<b>0.008</b>
		AFB1	$2.28 \times 10^{-5}$	$7.05 \times 10^{-5}$	0.323	0.748
		Time:AFB1	$8.17 \times 10^{-6}$	$4.71 \times 10^{-6}$	-1.735	0.087
		Intercept	0.141	0.0106	13.315	<b>&lt;0.001</b>
GIR <sub>mic</sub>		Time	-0.00065	0.000714	-0.91	0.366
		AFB1	$3.02 \times 10^{-5}$	$4.61 \times 10^{-5}$	0.654	0.515
		Time:AFB1	$-2.34 \times 10^{-6}$	$3.1 \times 10^{-6}$	-0.757	0.451
		Intercept	2.02	0.109	18.577	<b>&lt;0.001</b>
		Time	0.0292	0.00726	4.026	<b>&lt;0.001</b>
		AFB1	0.00126	0.000474	2.666	<b>0.009</b>
		Time:AFB1	$-8.49 \times 10^{-5}$	$3.17 \times 10^{-5}$	-2.682	<b>0.009</b>
GIR <sub>fun</sub>		Intercept	0.591	0.0533	11.09	<b>&lt;0.001</b>
		Time	-0.00327	0.0036	-0.909	0.366
		AFB1	0.000214	0.000233	0.922	0.359
		Time:AFB1	$6.93 \times 10^{-6}$	$1.56 \times 10^{-5}$	0.444	0.658
		Intercept	0.765	0.0349	21.905	<b>&lt;0.001</b>
		Time	-0.000799	0.00234	-0.342	0.733
		AFB1	0.000271	0.000152	1.776	0.08
sandy loam		Time:AFB1	$-1.24 \times 10^{-5}$	$1.02 \times 10^{-5}$	-1.214	0.228
		Intercept	0.215	0.0166	12.897	<b>&lt;0.001</b>
		Time	-0.00152	0.00112	-1.357	0.179
		AFB1	$8.7 \times 10^{-5}$	$7.26 \times 10^{-5}$	1.199	0.234
		Time:AFB1	$2.28 \times 10^{-6}$	$4.87 \times 10^{-6}$	0.468	0.641

**Table A3.** Cont.

Response	Soil	Predictor	B	SE	t	p
ERG:C <sub>mic</sub>	clay	Intercept	38.4	1.98	19.414	<0.001
		Time	0.42	0.132	3.182	0.002
		AFB1	0.0428	0.00862	4.964	<0.001
		Time:AFB1	-0.00178	0.000576	-3.097	0.002
	sandy loam	Intercept	0.0176	0.0011	15.998	<0.001
		Time	5.56 × 10 <sup>-5</sup>	6.81 × 10 <sup>-5</sup>	0.817	0.416
		AFB1	1.64 × 10 <sup>-6</sup>	4.8 × 10 <sup>-6</sup>	0.342	0.733
		Time:AFB1	5 × 10 <sup>-7</sup>	2.97 × 10 <sup>-7</sup>	1.684	0.095
BR <sub>fun</sub> :BR <sub>mic</sub>	clay	Intercept	0.671	0.0166	40.54	<0.001
		Time	-0.00138	0.00111	-1.251	0.215
		AFB1	-5.59 × 10 <sup>-5</sup>	7.23 × 10 <sup>-5</sup>	0.773	0.442
		Time:AFB1	-6.45 × 10 <sup>-6</sup>	4.83 × 10 <sup>-6</sup>	-1.335	0.186
	sandy loam	Intercept	0.623	0.0329	18.919	<0.001
		Time	0.00032	0.00223	0.144	0.886
		AFB1	-0.000109	0.000144	-0.755	0.452
		Time:AFB1	-1.57 × 10 <sup>-6</sup>	9.64 × 10 <sup>-6</sup>	-0.163	0.871
GIR <sub>fun</sub> :GIR <sub>mic</sub>	clay	Intercept	0.397	0.0159	24.961	<0.001
		Time	-0.00513	0.00106	-4.825	<0.001
		AFB1	-0.000111	6.94e-05	-1.595	0.115
		Time:AFB1	7.82 × 10 <sup>-6</sup>	4.64 × 10 <sup>-6</sup>	1.685	0.096
	sandy loam	Intercept	0.432	0.0362	11.932	<0.001
		Time	-0.00255	0.00244	-1.041	0.301
		AFB1	3.5e-05	0.000158	0.222	0.825
		Time:AFB1	-1.95 × 10 <sup>-6</sup>	1.06 × 10 <sup>-5</sup>	-0.184	0.855
BR <sub>mic</sub> :GIR <sub>mic</sub>	clay	Intercept	0.3	0.019	15.814	<0.001
		Time	-0.00524	0.00127	-4.125	<0.001
		AFB1	-0.000183	8.29 × 10 <sup>-5</sup>	-2.203	0.03
		Time:AFB1	6.16 × 10 <sup>-6</sup>	-5.54 × 10 <sup>-6</sup>	1.112	0.27
	sandy loam	Intercept	0.483	0.0466	10.361	<0.001
		Time	-0.00174	0.00315	-0.554	0.581
		AFB1	-1.38 × 10 <sup>-5</sup>	0.000203	-0.068	0.946
		Time:AFB1	-1.22 × 10 <sup>-5</sup>	1.36 × 10 <sup>-5</sup>	-0.896	0.373
BR <sub>fun</sub> :GIR <sub>fun</sub>	clay	Intercept	0.48	0.0223	21.585	<0.001
		Time	-0.00181	0.00149	-1.214	0.228
		AFB1	-0.000115	9.71 × 10 <sup>-5</sup>	-1.187	0.239
		Time:AFB1	-7.87 × 10 <sup>-6</sup>	6.49 × 10 <sup>-6</sup>	-1.212	0.229
	sandy loam	Intercept	0.687	0.039	17.609	<0.001
		Time	0.0027	0.00264	1.023	0.31
		AFB1	-0.000132	0.00017	-0.777	0.439
		Time:AFB1	-2.15 × 10 <sup>-5</sup>	1.14 × 10 <sup>-5</sup>	-1.88	0.064
qCO <sub>2,mic</sub>	clay	Intercept	-5.55	0.125	-44.546	<0.001
		Time	-0.0164	0.00833	-1.972	0.056
		AFB1	-0.000966	0.000544	-1.777	0.084
		Time:AFB1	2.03 × 10 <sup>-5</sup>	3.63 × 10 <sup>-5</sup>	0.559	0.58
	sandy loam	Intercept	0.00358	0.00033	10.85	<0.001
		Time	-6.1 × 10 <sup>-5</sup>	2.04 × 10 <sup>-5</sup>	-2.987	0.005
		AFB1	3.01 × 10 <sup>-6</sup>	1.44 × 10 <sup>-6</sup>	2.089	0.045
		Time:AFB1	-8.52 × 10 <sup>-8</sup>	8.9 × 10 <sup>-8</sup>	-0.957	0.346
qCO <sub>2,fun</sub>	clay	Intercept	0.0941	0.00426	22.092	<0.001
		Time	-0.000556	0.000285	-1.955	0.058
		AFB1	1.45 × 10 <sup>-5</sup>	1.86 × 10 <sup>-5</sup>	0.781	0.44
		Time:AFB1	-2.46 × 10 <sup>-6</sup>	1.24 × 10 <sup>-6</sup>	-1.984	0.055
	sandy loam	Intercept	0.109	0.00814	13.389	<0.001
		Time	-0.00122	0.000544	-2.244	0.031
		AFB1	1.53 × 10 <sup>-5</sup>	3.55 × 10 <sup>-5</sup>	0.429	0.67
		Time:AFB1	-2.19 × 10 <sup>-6</sup>	2.38 × 10 <sup>-6</sup>	-0.923	0.362

## Appendix E. Test Statistics of the Monte Carlo Permutation Test

**Table A4.** Test statistics of the Monte Carlo permutation test used to assess the significance of the effects of AFB1 concentration on the multivariate response (canonical coefficient of PRC). Significant results ( $p < 0.05$ ) are shown in bold.

Fraction	Soil	Day	DF	F	<i>p</i>
Microbial	sandy loam	0	1	0.26	0.838
		1	1	1.15	0.382
		3	1	2.36	0.105
		8	1	1.48	0.209
		15	1	0.13	0.838
		22	1	0.24	0.846
		28	1	2.7	0.117
	clay	0	1	1.51	0.21
		1	1	0.32	0.689
		3	1	5.36	<b>0.03</b>
		8	1	0.89	0.397
		15	1	0.03	0.997
Fungal	sandy loam	0	1	1.05	0.317
		1	1	2.4	0.109
		3	1	2.03	0.119
		8	1	1.08	0.324
		15	1	0.04	0.958
		22	1	1.13	0.314
		28	1	5.43	<b>0.013</b>
	clay	0	1	0.65	0.523
		1	1	0.11	0.911
		3	1	1.08	0.296
		8	1	1.06	0.344
		15	1	0.12	0.935
		22	1	0.56	0.479
		28	1	2.43	0.118

## Appendix F. Dissolved Organic Matter in Nonfumigated Samples

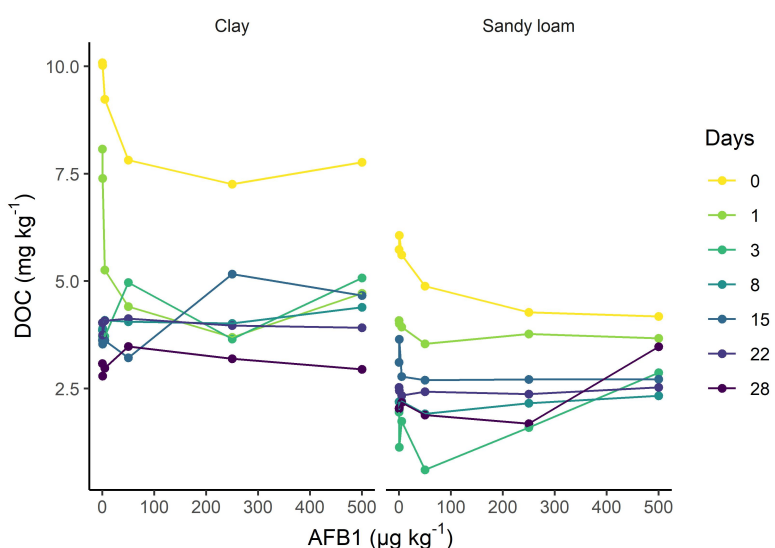


**Figure A7.** Dissolved organic carbon in the nonfumigated sandy loam and clay soils as a function of AFB1 concentration.

## References

- Accinelli, C.; Abbas, H.; Zablotowicz, R.; Wilkinson, J. *Aspergillus flavus* aflatoxin occurrence and expression of aflatoxin biosynthesis genes in soil. *Can. J. Microbiol.* **2008**, *54*, 371–379. [[CrossRef](#)] [[PubMed](#)]
- Horn, B.W. Ecology and population biology of aflatoxigenic fungi in soil. *J. Toxicol. Toxin Rev.* **2003**, *22*, 351–379. [[CrossRef](#)]
- Jaime-Garcia, R.; Cotty, P.J. *Aspergillus flavus* in soils and corncobs in south Texas: Implications for management of aflatoxins in corn-cotton rotations. *Plant Dis.* **2004**, *88*, 1366–1371. [[CrossRef](#)] [[PubMed](#)]
- Orum, T.V.; Bigelow, D.M.; Nelson, M.R.; Howell, D.R.; Cotty, P.J. Spatial and temporal patterns of *Aspergillus flavus* strain composition and propagule density in Yuma County, Arizona, soils. *Plant Dis.* **1997**, *81*, 911–916. [[CrossRef](#)]
- Abbas, H.; Wilkinson, J.; Zablotowicz, R.; Accinelli, C.; Abel, C.; Bruns, H.; Weaver, M. Ecology of *Aspergillus flavus*, regulation of aflatoxin production, and management strategies to reduce aflatoxin contamination of corn. *Toxin Rev.* **2009**, *28*, 142–153. [[CrossRef](#)]
- Elmholt, S. Mycotoxins in the soil environment. In *Secondary Metabolites in Soil Ecology*; Springer: Berlin/Heidelberg, Germany, 2008; pp. 167–203.
- Stoloff, L.; Dantzman, J.; Armbrecht, B. Aflatoxin excretion in wethers. *Food Cosmet. Toxicol.* **1971**, *9*, 839–846. [[CrossRef](#)]
- Fernández, A.; Belío, R.; Ramos, J.J.; Sanz, M.C.; Sáez, T. Aflatoxins and their metabolites in the tissues, faeces and urine from lambs feeding on an aflatoxin-contaminated diet. *J. Sci. Food Agric.* **1997**, *74*, 161–168. [[CrossRef](#)]
- Lüthy, J.; Zweifel, U.; Schlatter, C. Metabolism and tissue distribution of [<sup>14</sup>C] aflatoxin B<sub>1</sub> in pigs. *Food Cosmet. Toxicol.* **1980**, *18*, 253–256. [[CrossRef](#)]
- Stubblefield, R.; Pier, A.; Richard, J.; Shotwell, O. Fate of aflatoxins in tissues, fluids, and excrements from cows dosed orally with aflatoxin B<sub>1</sub>. *Am. J. Vet. Res.* **1983**, *44*, 1750–1752.
- Bardon, C.; Piola, F.; Bellvert, F.; Haichar, F.E.Z.; Comte, G.; Meiffren, G.; Pommier, T.; Pujalon, S.; Tsafack, N.; Poly, F. Evidence for biological denitrification inhibition (BDI) by plant secondary metabolites. *New Phytol.* **2014**, *204*, 620–630. [[CrossRef](#)]
- Zhang, Z.; Qiao, M.; Li, D.; Zhao, C.; Li, Y.; Yin, H.; Liu, Q. Effects of two root-secreted phenolic compounds from a subalpine coniferous species on soil enzyme activity and microbial biomass. *Chem. Ecol.* **2015**, *31*, 636–649. [[CrossRef](#)]
- Izhaki, I. Emodin—A secondary metabolite with multiple ecological functions in higher plants. *New Phytol.* **2002**, *155*, 205–217. [[CrossRef](#)]
- Fouché, T.; Claassens, S.; Maboeta, M. Aflatoxins in the soil ecosystem: An overview of its occurrence, fate, effects and future perspectives. *Mycotoxin Res.* **2020**, *36*, 303–309. [[CrossRef](#)]
- Wicklow, D.; Shotwell, O. Intrafungal distribution of aflatoxins among conidia and sclerotia of *Aspergillus flavus* and *Aspergillus parasiticus*. *Can. J. Microbiol.* **1983**, *29*, 1–5. [[CrossRef](#)] [[PubMed](#)]
- Weckbach, L.; Marth, E. Aflatoxin production by *Aspergillus parasiticus* in a competitive environment. *Mycopathologia* **1977**, *62*, 39–45. [[CrossRef](#)]
- Cuero, R.; Smith, J.; Lacey, J. Stimulation by *Hyphopichia burtonii* and *Bacillus amyloliquefaciens* of aflatoxin production by *Aspergillus flavus* in irradiated maize and rice grains. *Appl. Environ. Microbiol.* **1987**, *53*, 1142–1146. [[CrossRef](#)]
- Wicklow, D.; Hesseltine, C.; Shotwell, O.; Adams, G. Interference competition and aflatoxin levels in corn. *Phytopathology* **1980**, *78*, 68–74. [[CrossRef](#)]
- Burmeister, H.; Hesseltine, C. Survey of the sensitivity of microorganisms to aflatoxin. *Appl. Microbiol.* **1966**, *14*, 403–404. [[CrossRef](#)]
- Arai, T.; Ito, T.; Koyama, Y. Antimicrobial activity of aflatoxins. *J. Bacteriol.* **1967**, *93*, 59–64. [[CrossRef](#)]
- Angle, J.; Wagner, G. Aflatoxin B<sub>1</sub> effects on soil microorganisms. *Soil Biol. Biochem.* **1981**, *13*, 381–384. [[CrossRef](#)]
- Drott, M.T.; Debenport, T.; Higgins, S.A.; Buckley, D.H.; Milgroom, M.G. Fitness cost of aflatoxin production in *Aspergillus flavus* when competing with soil microbes could maintain balancing selection. *MBio* **2019**, *10*, e02782-18. [[CrossRef](#)] [[PubMed](#)]
- Pham, V.H.; Kim, J. Cultivation of unculturable soil bacteria. *Trends Biotechnol.* **2012**, *30*, 475–484. [[CrossRef](#)] [[PubMed](#)]
- Joergensen, R.G.; Emmerling, C. Methods for evaluating human impact on soil microorganisms based on their activity, biomass, and diversity in agricultural soils. *J. Plant Nutr. Soil Sci.* **2006**, *169*, 295–309. [[CrossRef](#)]
- Blagodatskaya, E.; Kuzyakov, Y. Active microorganisms in soil: Critical review of estimation criteria and approaches. *Soil Biol. Biochem.* **2013**, *67*, 192–211. [[CrossRef](#)]
- Anderson, J.P.; Domsch, K.H. A physiological method for the quantitative measurement of microbial biomass in soils. *Soil Biol. Biochem.* **1978**, *10*, 215–221. [[CrossRef](#)]
- Sassi, M.B.; Dollinger, J.; Renault, P.; Tlili, A.; Bérard, A. The FungiResp method: An application of the MicroResp™ method to assess fungi in microbial communities as soil biological indicators. *Ecol. Indic.* **2012**, *23*, 482–490. [[CrossRef](#)]
- Campbell, C.D.; Chapman, S.J.; Cameron, C.M.; Davidson, M.S.; Potts, J.M. A rapid microtiter plate method to measure carbon dioxide evolved from carbon substrate amendments so as to determine the physiological profiles of soil microbial communities by using whole soil. *Appl. Environ. Microbiol.* **2003**, *69*, 3593–3599. [[CrossRef](#)]
- Creamer, R.; Stone, D.; Berry, P.; Kuiper, I. Measuring respiration profiles of soil microbial communities across Europe using MicroResp™ method. *Appl. Soil Ecol.* **2016**, *97*, 36–43. [[CrossRef](#)]
- Creamer, R.E.; Bellamy, P.; Black, H.I.; Cameron, C.M.; Campbell, C.D.; Chamberlain, P.; Harris, J.; Parekh, N.; Pawlett, M.; Poskitt, J.; et al. An inter-laboratory comparison of multi-enzyme and multiple substrate-induced respiration assays to assess method consistency in soil monitoring. *Biol. Fertil. Soils* **2009**, *45*, 623–633. [[CrossRef](#)]

31. Anderson, J.; Domsch, K. Measurement of bacterial and fungal contributions to respiration of selected agricultural and forest soils. *Can. J. Microbiol.* **1975**, *21*, 314–322. [CrossRef] [PubMed]
32. Bailey, V.L.; Smith, J.L.; Bolton, H. Novel antibiotics as inhibitors for the selective respiratory inhibition method of measuring fungal: Bacterial ratios in soil. *Biol. Fertil. Soils* **2003**, *38*, 154–160. [CrossRef]
33. Kang, F.; Ge, Y.; Hu, X.; Goikavi, C.; Waigi, M.G.; Gao, Y.; Ling, W. Understanding the sorption mechanisms of aflatoxin B<sub>1</sub> to kaolinite, illite, and smectite clays via a comparative computational study. *J. Hazard. Mater.* **2016**, *320*, 80–87. [CrossRef] [PubMed]
34. Mertz, D.; Edward, T.; Lee, D.; Zuber, M. Absorption of aflatoxin by lettuce seedlings grown in soil adulterated with aflatoxin B<sub>1</sub>. *J. Agric. Food Chem.* **1981**, *29*, 1168–1170. [CrossRef]
35. Angle, J.; Wagner, G. Decomposition of aflatoxin in soil. *Soil Sci. Soc. Am. J.* **1980**, *44*, 1237–1240. [CrossRef]
36. Jaynes, W.; Zartman, R.; Hudnall, W. Aflatoxin B<sub>1</sub> adsorption by clays from water and corn meal. *Appl. Clay Sci.* **2007**, *36*, 197–205. [CrossRef]
37. Angle, J. Aflatoxin decomposition in various soils. *J. Environ. Sci. Health Part B* **1986**, *21*, 277–288. [CrossRef]
38. Goldberg, B.; Angle, J. *Aflatoxin Movement in Soil*; Technical report; Wiley Online Library: Hoboken, NJ, USA, 1985.
39. Albert, J.; Muñoz, K. Kinetics of microbial and photochemical degradation of aflatoxin B<sub>1</sub> in a sandy loam and clay soil. *Sci. Rep.* **2022**, *12*, 16849. [CrossRef]
40. OECD. 217. Soil Microorganisms: Carbon Transformation Test. In *OECD Guidelines for the Testing of Chemicals, Section 2*; OECD: Paris, France, 2000; Volume 2.
41. Starr, J.M.; Rushing, B.R.; Selim, M.I. Solvent-dependent transformation of aflatoxin B<sub>1</sub> in soil. *Mycotoxin Res.* **2017**, *33*, 197–205. [CrossRef] [PubMed]
42. Northcott, G.L.; Jones, K.C. Spiking hydrophobic organic compounds into soil and sediment: A review and critique of adopted procedures. *Environ. Toxicol. Chem. Int. J.* **2000**, *19*, 2418–2430. [CrossRef]
43. Vance, E.D.; Brookes, P.C.; Jenkinson, D.S. An extraction method for measuring soil microbial biomass C. *Soil Biol. Biochem.* **1987**, *19*, 703–707. [CrossRef]
44. Joergensen, R.G. The fumigation-extraction method to estimate soil microbial biomass: Calibration of the kEC value. *Soil Biol. Biochem.* **1996**, *28*, 25–31. [CrossRef]
45. Gong, P.; Guan, X.; Witter, E. A rapid method to extract ergosterol from soil by physical disruption. *Appl. Soil Ecol.* **2001**, *17*, 285–289. [CrossRef]
46. Campbell, C.; Grayston, S.; Hirst, D. Use of rhizosphere carbon sources in sole carbon source tests to discriminate soil microbial communities. *J. Microbiol. Methods* **1997**, *30*, 33–41. [CrossRef]
47. Banning, N.; Lalor, B.; Cookson, W.; Grigg, A.; Murphy, D. Analysis of soil microbial community level physiological profiles in native and post-mining rehabilitation forest: Which substrates discriminate? *Appl. Soil Ecol.* **2012**, *56*, 27–34. [CrossRef]
48. Degens, B.; Harris, J. Development of a physiological approach to measuring the catabolic diversity of soil microbial communities. *Soil Biol. Biochem.* **1997**, *29*, 1309–1320. [CrossRef]
49. Anderson, T.H.; Domsch, K.H. Soil microbial biomass: The eco-physiological approach. *Soil Biol. Biochem.* **2010**, *42*, 2039–2043. [CrossRef]
50. Anderson, T.H. Microbial eco-physiological indicators to asses soil quality. *Agric. Ecosyst. Environ.* **2003**, *98*, 285–293. [CrossRef]
51. Insam, H.; Öhlinger, R. Ecophysiological parameters. In *Methods in Soil Biology*; Springer: Berlin/Heidelberg, Germany, 1996; pp. 306–309.
52. Wickham, H.; Averick, M.; Bryan, J.; Chang, W.; McGowan, L.D.; François, R.; Grolemund, G.; Hayes, A.; Henry, L.; Hester, J.; et al. Welcome to the Tidyverse. *J. Open Source Softw.* **2019**, *4*, 1686. [CrossRef]
53. Oksanen, J.; Blanchet, F.G.; Kindt, R.; Legendre, P.; Minchin, P.R.; O’hara, R.; Simpson, G.L.; Solymos, P.; Stevens, M.H.H.; Wagner, H.; et al. Package ‘vegan’. *Community Ecol. Packag. Version* **2013**, *2*, 1–295.
54. Steinmetz, Z.; Albert, J.; Kenngott, K. Envalysis: Miscellaneous Functions for Environmental Analyses. R Package Version 0.5.4; 2022. Available online: <https://cran.r-project.org/package=envalysis> (accessed on 20 January 2023).
55. Zuur, A.F.; Ieno, E.N.; Elphick, C.S. A protocol for data exploration to avoid common statistical problems. *Methods Ecol. Evol.* **2010**, *1*, 3–14. [CrossRef]
56. Montgomery, D.C.; Peck, E.A.; Vining, G.G. *Introduction to Linear Regression Analysis*; John Wiley & Sons: Hoboken, NJ, USA, 2012.
57. Wakelin, S.; Lombi, E.; Donner, E.; MacDonald, L.; Black, A.; O’Callaghan, M. Application of MicroResp™ for soil ecotoxicology. *Environ. Pollut.* **2013**, *179*, 177–184. [CrossRef] [PubMed]
58. Leys, C.; Ley, C.; Klein, O.; Bernard, P.; Licata, L. Detecting outliers: Do not use standard deviation around the mean, use absolute deviation around the median. *J. Exp. Soc. Psychol.* **2013**, *49*, 764–766. [CrossRef]
59. Box, G.E.; Cox, D.R. An analysis of transformations. *J. R. Stat. Soc. Ser. (Methodol.)* **1964**, *26*, 211–243. [CrossRef]
60. Van den Brink, P.J.; Ter Braak, C.J. Multivariate analysis of stress in experimental ecosystems by principal response curves and similarity analysis. *Aquat. Ecol.* **1998**, *32*, 163–178. [CrossRef]
61. Van den Brink, P.J.; Braak, C.J.T. Principal response curves: Analysis of time-dependent multivariate responses of biological community to stress. *Environ. Toxicol. Chem. Int. J.* **1999**, *18*, 138–148. [CrossRef]
62. Frampton, G.K.; Van den Brink, P.J.; Gould, P.J. Effects of spring precipitation on a temperate arable collembolan community analysed using Principal Response Curves. *Appl. Soil Ecol.* **2000**, *14*, 231–248. [CrossRef]

63. Szöcs, E.; Van den Brink, P.J.; Lagadic, L.; Caquet, T.; Roucaute, M.; Auber, A.; Bayona, Y.; Liess, M.; Ebke, P.; Ippolito, A.; et al. Analysing chemical-induced changes in macroinvertebrate communities in aquatic mesocosm experiments: A comparison of methods. *Ecotoxicology* **2015**, *24*, 760–769. [[CrossRef](#)] [[PubMed](#)]
64. Mori, T.; Wang, S.; Wang, C.; Mo, J.; Zhang, W. Is microbial biomass measurement by the chloroform fumigation extraction method biased by experimental addition of N and P? *iForest-Biogeosci. For.* **2021**, *14*, 408. [[CrossRef](#)]
65. Schenzel, J.; Goss, K.U.; Schwarzenbach, R.P.; Bucheli, T.D.; Droge, S.T. Experimentally determined soil organic matter–water sorption coefficients for different classes of natural toxins and comparison with estimated numbers. *Environ. Sci. Technol.* **2012**, *46*, 6118–6126. [[CrossRef](#)]
66. Ahmed, A.A.; Thiele-Bruhn, S.; Aziz, S.G.; Hilal, R.H.; Elroby, S.A.; Al-Youbi, A.O.; Leinweber, P.; Kühn, O. Interaction of polar and nonpolar organic pollutants with soil organic matter: Sorption experiments and molecular dynamics simulation. *Sci. Total Environ.* **2015**, *508*, 276–287. [[CrossRef](#)] [[PubMed](#)]
67. Zhu, D.; Hyun, S.; Pignatello, J.J.; Lee, L.S. Evidence for  $\pi$ - $\pi$  electron donor-acceptor interactions between  $\pi$ -donor aromatic compounds and  $\pi$ -acceptor sites in soil organic matter through pH effects on sorption. *Environ. Sci. Technol.* **2004**, *38*, 4361–4368. [[CrossRef](#)]
68. Manrique, L.; Jones, C.; Dyke, P. Predicting cation-exchange capacity from soil physical and chemical properties. *Soil Sci. Soc. Am. J.* **1991**, *55*, 787–794. [[CrossRef](#)]
69. Manzoni, S.; Taylor, P.; Richter, A.; Porporato, A.; Ågren, G.I. Environmental and stoichiometric controls on microbial carbon-use efficiency in soils. *New Phytol.* **2012**, *196*, 79–91. [[CrossRef](#)] [[PubMed](#)]
70. Öquist, M.G.; Erhagen, B.; Hæi, M.; Sparrman, T.; Ilstedt, U.; Schleucher, J.; Nilsson, M.B. The effect of temperature and substrate quality on the carbon use efficiency of saprotrophic decomposition. *Plant Soil* **2017**, *414*, 113–125. [[CrossRef](#)]
71. Jones, D.; Edwards, A. Influence of sorption on the biological utilization of two simple carbon substrates. *Soil Biol. Biochem.* **1998**, *30*, 1895–1902. [[CrossRef](#)]
72. Jiang, D.; Huang, Q.; Cai, P.; Rong, X.; Chen, W. Adsorption of *Pseudomonas putida* on clay minerals and iron oxide. *Colloids Surf. B Biointerfaces* **2007**, *54*, 217–221. [[CrossRef](#)]
73. Tietjen, T.; Wetzel, R.G. Extracellular enzyme-clay mineral complexes: Enzyme adsorption, alteration of enzyme activity, and protection from photodegradation. *Aquat. Ecol.* **2003**, *37*, 331–339. [[CrossRef](#)]
74. Kaiser, K.; Zech, W. Competitive sorption of dissolved organic matter fractions to soils and related mineral phases. *Soil Sci. Soc. Am. J.* **1997**, *61*, 64–69. [[CrossRef](#)]
75. Beck, M.; Robarge, W.; Buol, S. Phosphorus retention and release of anions and organic carbon by two Andisols. *Eur. J. Soil Sci.* **1999**, *50*, 157–164. [[CrossRef](#)]
76. Hadacek, F.; Bachmann, G.; Engelmeier, D.; Chobot, V. Hormesis and a chemical raison d’être for secondary plant metabolites. *Dose Response* **2011**, *9*, 79–116. [[CrossRef](#)]
77. Hashmi, M.Z.; Shen, H.; Zhu, S.; Yu, C.; Shen, C. Growth, bioluminescence and shoal behavior hormetic responses to inorganic and/or organic chemicals: A review. *Environ. Int.* **2014**, *64*, 28–39. [[CrossRef](#)] [[PubMed](#)]
78. Finotti, E.; Parroni, A.; Zaccaria, M.; Domin, M.; Momeni, B.; Fanelli, C.; Reverberi, M. Aflatoxins are natural scavengers of reactive oxygen species. *Sci. Rep.* **2021**, *11*, 16024. [[CrossRef](#)]
79. Fierer, N.; Jackson, J.A.; Vilgalys, R.; Jackson, R.B. Assessment of soil microbial community structure by use of taxon-specific quantitative PCR assays. *Appl. Environ. Microbiol.* **2005**, *71*, 4117–4120. [[CrossRef](#)] [[PubMed](#)]
80. Frostegård, Å.; Tunlid, A.; Bååth, E. Microbial biomass measured as total lipid phosphate in soils of different organic content. *J. Microbiol. Methods* **1991**, *14*, 151–163. [[CrossRef](#)]
81. Frostegård, Å.; Tunlid, A.; Bååth, E. Use and misuse of PLFA measurements in soils. *Soil Biol. Biochem.* **2011**, *43*, 1621–1625. [[CrossRef](#)]

**Disclaimer/Publisher’s Note:** The statements, opinions and data contained in all publications are solely those of the individual author(s) and contributor(s) and not of MDPI and/or the editor(s). MDPI and/or the editor(s) disclaim responsibility for any injury to people or property resulting from any ideas, methods, instructions or products referred to in the content.